Moreiro, I.S., Moreira-Turcq, P., Kim, J.-H., Turcq , B., Cordeiro, R.C., Caquineau, S., Mandengo-Yogo, M. & Sinninghe Damsté, J.S. (2014). A mineralogical and organic geochemical overview of the effects of Holocene changes in Amazon River flow on three floodplain lakes. Palaeogeography, Palaeoclimatology, Palaeoecology, 415, 152–164

Published version: dx.doi.org/10.1016/j.palaeo.2014.03.017

Link NIOZ Repository: www.vliz.be/nl/imis?module=ref&refid=243686

[Article begins on next page]

A Mineralogical and Organic Geochemical Overview of the Effects of Holocene Changes in Amazon River Flow on Floodplain Lakes

Moreira, L. S.[1,*]; Moreira-Turcq, P.[2]; Kim, J.-H.[3]; Turcq, B.[4]; Cordeiro, R. C.[1]; Caquineau, S.[4]; Mandengo-Yogo, M.[4]; Sinninghe Damsté, J. S.[3]

[1]Departamento de Geoquímica, Universidade Federal Fluminense (UFF), Niterói, Brazil

[2]Institut de Recherche pour Développement (IRD) – GET (Géosciences Environment Toulouse), Bondy, France

[3]NIOZ Royal Netherlands Institute for Sea Research, NL-1790 AB Den Burg, the Netherlands

[4]Institut de Recherche pour Développement (IRD) – LOCEAN (Laboratoire d'Océanographie et du Climat), Bondy, France

*Corresponding author:

E-mail address: lucianebiouff@gmail.com

ABSTRACT

A synthesis of the impacts of the Amazon River hydrological changes on the sedimentation process of organic matter (OM) in three different floodplain lakes (Santa Ninha, Maracá, and Comprido lakes) is presented in this study. Today the Santa Ninha and Maracá lakes are directly and permanently connected with the main channel of the Amazon River, in contrast to Comprido Lake, which is indirectly and periodically influenced by the Amazon River due to its high distance from the main channel. All the sedimentary lake records showed a reduced river inflow due to dry climatic conditions during the Early and Middle Holocene followed by a humid Late Holocene with an increased fluvial input. In Santa Ninha and Maraca Lakes the reduced river inflow period was characterized by sediments with a low abundance of smectite (on average ~20 wt. %), a clay mineral mainly transported by the fluvial system, high total organic carbon (TOC) contents (on average ~8.2 wt. %) and a predominant acidic soil OM input evidenced by high branched glycerol dialkyl glycerol tetraethers (GDGT) concentrations (on average 180 µg g_{TOC}^{-1}). During the Late Holocene, a higher smectite abundance (on average ~43 wt. %) and a low TOC content (on average ~1.4 wt. %) pointed to dilution with the riverine lithogenic matter. This was accompanied by a proportional increase in the aquatically-produced crenarchaeol, suggesting an increased lake water level. In Comprido Lake, a sedimentation gap occurred during the Early and Middle Holocene. The humid Late Holocene, after 3,000 cal years BP, was characterized by high TOC values (on average ~9 wt. %) as well as a sharp increase in soil OM input as revealed by the increase in branched GDGT concentrations (on average ~81 µg g_{TOC}^{-1}), but the smectite content was low (on average ~14 %). This suggests that in Comprido Lake the soil OM input from the local catchment area was predominant during the humid Late Holocene due to its high distance from the Amazon

River main stem. Consequently, our study shows that the sedimentation processes of OM in Amazonian floodplain lakes are strongly influenced by variations in the hydrodynamic regime of the Amazon River during the Holocene. However, its impacts on floodplain lakes were different, mainly depending on the distance from the main stem of the Amazon River.

Keywords: sedimentary organic matter; glycerol dialkyl glycerol tetraethers; Amazonian floodplain lakes; Holocene

1. Introduction

A study of sedimentation process allows a better understanding of the driving forces and impacts of past climate change on the ecosystems (Jones et al., 2009). In the Amazonian Basin, pollen, microscopic charcoal, and geochemical data have been used to determine the relationship between vegetation dynamics and climate changes during the Holocene (Absy,1974; Sifeddine et al., 1994, 2001; Cordeiro et al., 1997, 2008, 2011; Turcq et al.,1998; Behling and Hooghiemstra, 1999; Behling et al., 2001; Weng et al., 2006; Bush et al., 2007; De Toledo and Bush, 2007; Hillyer et al. 2009; Hermanowski et al., 2012; Moreira et al., 2012, 2013a,b). These studies indicated that the climatic conditions in the Amazon Basin during the Early and Middle Holocene were much drier (e.g. Hermanowski et al., 2012; Mayle and Power, 2008; Cordeiro et al., 2008; Sifeddine et al., 1998, 2001; Mayle, 2000; Absy, 1979) and a transition to a wettest climate was observed in the Late Holocene (e.g. Cordeiro et al., 2008; Bush et al., 2007; Behling and Costa, 2000). However, much of the Amazon paleoenvironmental history has been derived from studies of lakes isolated from the hydrological dynamics of the Amazon Basin. Despite of the large area of the floodplains, which occupy approximately 44 % of the Amazon Basin (Guyot et al., 2007), and their connection with the Amazon River, the paleoclimatic impacts on the floodplain sedimentation is limited.

In order to understand the Amazon River influence on Amazonian floodplain lakes during the Holocene and its impacts on changes of sedimentary organic matter (OM) sources, a comparison of the organic and mineralogical parameters was conducted by Moreira et al. (2012, 2013a,b) in three different floodplain lakes. The authors showed that the Amazon River hydrological variations exercised an important impact on the sedimentation process in floodplain lakes, reflected by the records of erosive events and variations in the total organic carbon (TOC) content and its stable carbon isotopic composition. These variations were accompanied by changes in the mineralogical composition that markedly indicated the variations of the Amazon River influence on floodplain lakes and allowed the determination of periods of lower and higher sediment input of particles from the Amazon River into the floodplain lakes. In addition, the Amazon River paleohydrological variations presented different impacts on floodplain lakes depending on the distance from the main channel. For instance, Comprido Lake, located in the eastern central Amazon Basin, has been indirectly but constantly under the influence of the Amazon River and its sedimentary record provided information on regional Holocene climate changes (Moreira et al., 2013a). In contrast, the sedimentary records from lakes closer to the main stem of the Amazon River, such as Maracá Lake (Moreira et al., 2013b) and Santa Ninha Lake (Moreira et al., 2012) presented a series of erosive events during the Holocene as a consequence of the hydrological variations of the Amazon River. However, the sources of the sedimentary OM in those lakes are still poorly understood.

Although Santa Ninha, Maracá, and Comprido Lakes were previously studied (Moreira et al., 2012, 2013a,b), a comprehensive comparison of these lakes have not been performed yet. In this study, we, therefore, synthesize the previous results for a direct comparison between the different types of floodplain lakes in order to better understand the sources and the sedimentation processes of OM in these lakes and their links to the hydrological variations of the Amazon River during the Holocene. In addition to the previously published data, we newly obtained Holocene records of the concentrations and distributions of crenarchaeol and branched glycerol dialkyl glycerol tetraethers (GDGTs) from Santa Ninha and Comprido Lakes, complementing our recent efforts on paleohydrological and paleoclimatic reconstructions in Amazonian floodplain lakes.

2. Study area

Santa Ninha Lake is located in Várzea do Lago Grande de Curuai, a complex floodplain system of more than 30 interconnected lakes, all permanently connected to the Amazon main stem by small channels. This floodplain is situated between 1°50'S–02°15'S and 55°00'W–56°05'W on the southern margin of the Amazon River, at 850 km from the Amazon River mouth (Fig. 1). The northern limit of Curuai floodplain is formed by river banks. Southwards the 'terra firme' forest is located on elevated terrain with dense forest (Martinez and Le Toan, 2007). Around the lakes the pioneer formations are dominated by *Echinochloa polystachya*, *Paspalum repens*, and *Paspalum fasciculatum as* C_4 plants and *Salvínea auriculata, Pistia stratiotes,* and *Eichornia crassipes* as C_3 plants.

Maracá and Comprido Lakes are situated between 54º0'W-53º52'W and 02º8'S-02º16'S. This floodplain system is near the city of Monte Alegre on the south bank of the Amazon River at 500 km from the Amazon River mouth. Maracá Lake is characterized by a direct and permanent connection with the Amazon River throughout the year. In contrast, Comprido Lake is completely isolated during low water phases. Both lakes are surrounded by a dense tropical rain forest (terra firme forest) in the southern bank, and a forest-savanna transition in the northern bank (Radambrasil, 1974). Around the lakes there are also pioneer formations (grasslands) with the predominance of *Paspalum fasciculatum*, *Paspalum repens*, *Echinochloa polystachya* (C_4 plants), and *Eichornia crassipes* (a C_3 plant).

In the catchments of Santa Ninha, Maracá and Comprido Lakes the bedrock of the terra firme (i.e. unflooded upland) comprises the Cretaceous Alter do Chão Formation (Latrubesse et al., 2009) which is a succession of feldspathic-kaolinitic sandstones, conglomerates and mudstones (Nogueira and Sarges, 2001; Mendes et al., 2012). The main clay mineral delivered by terra firme creeks is predominantly kaolinite (Behling et al., 2001; Guyot el al., 2007; Amorim, 2010). The catchment area is characterized by a humid tropical climate without long dry periods. The annual mean precipitation is about 2200 mm and the annual mean air temperature is about 27°C (Radambrasil, 1974).

3. Methods

3.1. Sediment cores

The TA14 core was collected in Santa Ninha Lake (S02°07'31.2" and W55°49'29") using a ‘‘vibra-core’’. The MAR2 and COM1 cores were collected manually in Maracá and Comprido Lake at S02°10'14.3"/W053°55'57.4" and S02°12'18.5"/W53°54'01.8", respectively (Fig. 1). The cores were opened, described and sampled in the Laboratory at Universidade Federal Fluminense, Niteroi, Brazil.

3.2. Radiocarbon (^{14}C) analysis

The ^{14}C measurements were performed on TOC by an Artemis accelerator mass spectrometry (AMS) system based on a 3MV Pelletron from National Electrostatics Corporation (NEC, Middleton, Wisconsin, USA) at Laboratoire de Mesure du Carbone 14 (LMC14) - UMS 2572 (CEA/DSM CNRS IRD IRSN – Ministère de la Culture et de la Communication), Paris, France. To consistently establish chronologies for three sediment cores, the calibrated ages were newly obtained using the CALIB 7.0, available at http://radiocarbon.pa.qub.ac.uk/calib (Stuiver et al., 1998) and the calibration curve used was SHcal13 (Hogg et al., 2013). In order to obtain age-depth models the software *'Bacon'*, version 2.2 (Blaauw and Christen, 2011) was used.

3.3. Clay mineral and bulk OM analysis

Clay mineralogy, TOC, total nitrogen (TN) and stable isotopic compositions of TOC ($\delta^{13}C_{TOC}$) were determined as described by Moreira et al. (2012, 2013a,b).

3.4. GDGT analysis and calculation of indices

Freeze-dried samples were extracted with an Accelerated Solvent Extractor (DIONEX ASE 200) using a mixture of dichloromethane (DCM): methanol (MeOH, 9:1 v:v). The extract was separated into apolar, ketone, and polar fractions over an Al_2O_3 column using hexane:DCM (9:1 v:v), hexane:DCM (1:1 v:v), and DCM:MeOH (1:1 v:v), respectively. The polar fractions (DCM:MeOH, 1:1 v:v) were analyzed for GDGTs according to the procedure described by Schouten et al. (2007). The polar fractions were dried down under nitrogen, re-dissolved by sonication (5 min) in hexane:propanol (99:1 v:v), and filtered through 0.45 μm polytetrafluoroethylene (PTFE) filters. The samples were analysed using high performance liquid chromatography-atmospheric pressure positive ion chemical ionization mass spectrometry (HPLC-APCI-MS). GDGTs were detected by selected ion monitoring of their $(M+H)^+$ ions (dwell time 237 ms) and quantification of the GDGT compounds was achieved by integrating the peak areas and using the C_{46} GDGT internal standard according to Huguet et al. (2006).

In order to quantify the different GDGT distributions along the cores, the branched and isoprenoid tetraether (BIT) index (Hopmans et al., 2004), the methylation index of branched tetraethers (MBT) (Weijers et al., 2007), the cyclization ratio of branched tetraethers (CBT) (Weijers et al., 2007), and the degree of cyclization (DC) (Sinninghe Damsté et al., 2009) were calculated as follows:

$$\text{BIT index} = \frac{[\text{Ia}]+[\text{IIa}]+[\text{IIIa}]}{[\text{Ia}]+[\text{IIa}]+[\text{IIIa}]+[\text{IV}]} \quad (1)$$

$$\text{MBT} = \frac{[\text{Ia}]+[\text{Ib}]+[\text{Ic}]}{[\text{Ia}]+[\text{Ib}]+[\text{Ic}]+[\text{IIa}]+[\text{IIb}]+[\text{IIc}]+[\text{IIIa}]+[\text{IIIb}]+[\text{IIIc}]} \quad (2)$$

$$\text{CBT} = -\log\left(\frac{[\text{Ib}]+[\text{IIb}]}{[\text{Ia}]+[\text{IIa}]}\right) \quad (3)$$

$$\text{DC} = \frac{[\text{Ib}]+[\text{IIb}]}{[\text{Ia}]+[\text{Ib}]+[\text{IIa}]+[\text{IIb}]} \quad (4)$$

The roman numerals refer to the GDGTs indicated in Fig. 2. Ia-c, IIa-c, and IIIa-c are branched GDGTs and IV is the isoprenoid GDGT, crenarchaeol. For the calculation of the CBT-derived pH and the MBT/CBT-derived mean annual air temperature (MAAT), the regional soil calibrations for the Amazon Basin were used (Bendle et al., 2010):

$$\text{CBT} = 4.2313 - 0.5782 \times \text{pH} \; (r^2 = 0.75) \quad (5)$$

$$\text{MBT} = 0.1874 + 0.0829 \times \text{CBT} + 0.0250 \times \text{MAAT} \; (r^2 = 0.91) \quad (6)$$

4. Results

4.1. Chronology and lithology

The AMS ^{14}C data of the sediment cores investigated were summarized in Table 1 and the age–depth models were illustrated in Fig. 3. The TA14 chronological model was based on fourteen TOC AMS radiocarbon dates and showed a basal age of 5,600 cal years BP (Moreira et al., 2012). The MAR2 age-depth model was constructed with seven TOC AMS radiocarbon dates and presented a basal age of 3,600 cal years BP (Moreira et al., 2013b). The COM1 chronology was based on seven TOC AMS radiocarbon dates and showed a basal age of 10,300 cal years BP (Moreira et al., 2013a).

The TA14 (Santa Ninha Lake) and MAR2 (Maracá Lake) sediment cores mainly consisted of clay (Fig. 4). The base of core TA14 (270-165 cm), according to the visual lithological inspection, was composed by thin horizontal laminations of dark grey clay and plant remains (Moreira et al., 2012, 2013b) and contained high amounts of TOC (>10 wt. %; Fig. 5). A sharp contact was identified at 34 cm. A transition to a dark greyish-brown silty-clay layer without plant remains was found in the following units until the top. The base of MAR2 (86-72 cm) was also composed by organic-rich clay layers (Fig. 4) and in the rest of the core, no vegetal remains were found, except at the base of this core (Fig. 4). A sharp contact due to strong erosive events can also be observed in this core, at 35.5 cm and 51.5 cm. In the COM1 core (Fig. 4), from the base to 95 cm, the sediment was characterized by the presence of very dark grey clay, without vegetal remains (Moreira et al., 2013a) and a low TOC content (Fig. 5). In the following units, a predominantly organic rich clay layer with vegetal remains was found on the top of COM1 core.

In the three sediment cores, two distinct periods were observed. A period with low river influence, classified as Unit II, occurred between 5,600 and 5,000 cal years BP in Santa Ninha Lake, between 3,600 and 2,700 cal years BP in Maracá Lake, and between 10,300 and 3,000 cal years BP in Comprido Lake. A transition to a period with high river input into the lakes was evidenced since the Late Holocene. This period corresponds to Unit I which occurred during the last 5,000 years in Santa Ninha Lake, during the last 2,700 years in Maracá Lake, and since the last 3,000 years in Comprido Lake. These units and their mean values of the mineralogical and organic geochemistry results are discussed below.

4.2. Mineralogical characterization

The kaolinite content in the Unit II of TA14 and MAR2 cores presented an average of 40 % and 73.8 %, respectively, which decreased in the Unit I, with mean values of 27.8 % and 39 %, respectively. In contrast, the smectite content in the Unit II of both TA14 and MAR2 cores was low, with mean values of 25.1 % and 6.8 %, respectively, while the Unit II showed a substantial increase, with mean values of 43.2 % and 42.7 %, respectively (Fig. 5). For more details, the mineralogical characterization of the TA14 and MAR2 cores were presented by Moreira et al. (2012, 2013b). In COM1 core, the predominance of kaolinite occurred along the record, with the mean value of 53.8 %, while the smectite content presented the mean value of 14.5 %, with the peak value of 25 % (Fig.6), as described by Moreira et al. (2013a).

4.3. Characterization of the bulk OM

In Santa Ninha Lake (TA14), the Unit II was characterized by high TOC values and C:N atomic ratios, with the mean values of 8.2 wt. % and 23, respectively (Figs. 5-6). A decrease in TOC values and C:N atomic ratio can be observed in the Unit I, with an average of 0.48 wt. % and 4.3, respectively. The mean value of $\delta^{13}C_{TOC}$ during the Unit II was -28.7 ‰ and during the Unit I the carbon isotopic compositions were heavier than the other periods but no significant variations were observed after 4,000 cal years BP, as described by Moreira et al. (2012).

In the Unit II of MAR2 core the mean values of TOC and C:N atomic ratios were 15.3 wt. % and 23, respectively (Figs. 5-6). The mean values of TOC and C:N atomic ratio for the Unit I were 2.3 wt. % and 14, respectively. The $\delta^{13}C_{TOC}$ values in the Unit II presented an average of -25.8 ‰, while the Unit I had enriched $\delta^{13}C_{TOC}$ values, with an average of -20.5 ‰. After 1880 cal years BP, the mean value of $\delta^{13}C_{TOC}$ was -27 ‰ as described by Moreira et al. (2013b).

The Unit II in COM1 core showed the lowest TOC content and C:N atomic ratio with the mean values of 0.4 wt. % and 5.6, respectively (Figs. 5-6). These values gradually increased toward the core top and the mean values of the Unit I were 9.3 wt. % and 14.3, respectively. A large increase in $\delta^{13}C_{TOC}$ was observed between 9,300 and 8,600 cal years BP, ranging from -23.7 ‰ to -17.6 ‰. After this period, $\delta^{13}C_{TOC}$ values were lower, with the mean value of -28.4 ‰. Moreira et al. (2013a) provide more detailed characterization of the bulk OM for COM1 core.

4.4. GDGT concentration and distribution

In general, the GDGT Ia was the most abundant branched GDGT in all the lake sediments analysed and followed by the GDGT Ib and IIa with similar proportions. The GDGT IIIb and IIIc were mostly absent, which is consistent with the finding that these compounds were not detected in 63 % of the global surface soil set (Peterse et al., 2012) and in most of Amazon soils (Zell et al., 2013a).

In the Unit II of TA14 core from Santa Ninha Lake, the concentrations of crenarchaeol and the summed branched GDGTs varied between 0.6 and 4 µg g_{TOC}^{-1} and between 37 and 130 µg g_{TOC}^{-1}, respectively (Fig. 5). Note that the summed branched GDGTs were calculated as the sum of the concentrations of the major three branched GDGTs, i.e. GDGT Ia, IIa, and IIIa. The BIT index was the highest during this period, varying between 0.94 and 0.98, similar to that reported for Amazonian soils (Kim et al., 2012; Zell et al., 2013a). The DC (Sinninghe Damsté et al., 2009) ranged from 0.02 to 0.05 and the CBT-derived pH followed the pattern of the DC, with the values of 4-5 (Fig. 7). The MBT/CBT–derived MAAT in this phase varied between 23.9 and 26.4ºC and followed the pattern of the MBT (Fig. 7). The Unit I revealed a decrease in the concentrations of summed branched GDGTs, ranging from 7 to 90 μg g_{TOC}^{-1}. In contrast, the concentrations of crenarchaeol reached the highest value during this period, up to 18 μg g_{TOC}^{-1}. The BIT index revealed substantial variations, ranging from 0.77 to 0.97. The DC ranged from 0.06 to 0.31 and the CBT-derived pH presented high values than the Unit II, varying between 5.3 and 6.4. The MBT/CBT–derived MAAT varied between 21.6 and 26.4 ºC and also followed the pattern of the MBT.

In Maracá Lake (MAR2) the concentrations of crenarchaeol and the summed branched GDGTs in the Unit II varied between 4 and 13 μg g_{TOC}^{-1} and between 370 and 900 μg g_{TOC}^{-1}, respectively (Fig. 5). The BIT index was high and no variation was detected in this phase, with a mean value of 0.99, ranging between 0.98 and 0.99 (Fig. 5). The MBT and the DC also revealed low variations during this period, with the mean values of 0.97 (ranging from 0.97 to 0.96) and 0.02 (ranging from 0.01 to 0.03), respectively (Fig. 7). The CBT-derived pH and MBT/CBT–derived MAAT also presented low variations during this period, with mean values of 4.4 (varying between 4.1 and 4.7) and 25.6 ºC (varying between 25.2 ºC and 26.1 ºC), respectively (Fig. 7). In the Unit I, the crenarchaeol contribution to the sedimentary GDGT pool increased and consequently a slight reduction of the BIT values (ranging from 0.92 to 0.98) occurred. In this unit, a reduction in the summed branched GDGT concentration was also observed, varying between 34 and 130 μg g_{TOC}^{-1}. A significant increase in the DC and CBT-derived pH occurred during this period, ranging from 0.03 to 0.28 and 4.8 to 6.4, respectively. The MBT/CBT–derived MAAT presented a slight decrease varying between 23.1 and 25.8ºC.

In COM1 core, extremely low concentrations of crenarchaeol and summed branched GDGTs were found in the Unit II, with mean values of 0.01 μg g_{TOC}^{-1} (varying between 0.007 and 0.02 μg g_{TOC}^{-1}) and 0.4 μg g_{TOC}^{-1} (varyging between 0.3 and 0.4 μg g_{TOC}^{-1}), respectively (Fig. 5). The BIT index was an average of 0.98 without large variations, ranging from 0.96 to 0.98 (Fig. 5). The MBT and the DC, in the Unit II, also showed low variations with the averages of 0.89 (ranging between 0.87 and 0.91) and 0.06 (varying between 0.05 and 0.06), respectively (Fig. 7). The values of CBT-derived pH and MBT/CBT–derived temperatures also presented low variations with an average of 5.2 and 24 ºC, respectively (Fig. 7). During the last 3,000 cal years BP, a significant increase in the summed branched GDGT concentrations was observed, with the minimum of 39 μg g_{TOC}^{-1} and the maximum of 110 μg g_{TOC}^{-1}, with an average of 81.4 μg g_{TOC}^{-1}. The concentrations of crenarchaeol for the last 3,000 cal years BP were low when compared with the other records. However, a slight increase occurred, ranging from 0.3 to 2 μg g_{TOC}^{-1}, with higher values during the last 300 cal years BP. The BIT index was constant with mean value of 0.99. The MBT and the DC, after 3,000 cal years BP, showed mean values of 0.92 (ranging from 0.87 to 0.94) and 0.07 (ranging from 0.03 to 0.12), respectively. The CBT-derived pH and MBT/CBT–derived temperatures varied between 4.7 and 5.7 and between 24.4 and 26 ºC, respectively.

5. Discussion

In the floodplain lakes located in the central Amazon Basin, we carried out a multi-proxy study, effectively combining mineralogical data with organic geochemical data. The Amazon River sediments have a clay assemblage characterized by relatively high smectite content (Guyot et al., 2007). In contrast, kaolinite is the main clay mineral in the catchment areas of the lowland Amazon Basin (Behling et al., 2001; Guyot el al., 2007; Amorim, 2010). Hence, variations in the clay assemblage in the floodplain lake sediments are linked to changes in the sediment supply sources into the studied lakes, i.e. the Amazon River versus the local catchment area. Besides the clay assemblage, the carbon elemental and isotopic composition as well as a number of parameters based on crenarchaeol and branched GDGTs were applied to characterize the OM sources and to reconstruct pH and MAAT. Crenarchaeol is considered to be the specific membrane-spanning lipid of aquatic planktonic Thaumarchaeota (e.g. Sinninghe Damsté et al., 2002; Pitcher et al., 2011), formerly known as Group I Crenarchaeota (Spang et al., 2010). Recent studies in the central Amazon Basin showed that crenarchaeol is mainly produced in the aquatic system, with relatively low amounts in soils (Kim et al., 2012; Zell et al., 2013a,b). Branched GDGTs are ubiquitous and dominant in peats (e.g. Sinninghe Damsté et al., 2000; Weijers et al., 2004, 2006) and soils (e.g. Weijers et al., 2007; Kim et al., 2007, 2010), probably derived from anaerobic (e.g. Weijers et al., 2006) and heterotrophic (e.g. Pancost and Sinninghe Damsté, 2003; Weijers et al., 2010) acidobacteria (e.g. Weijers et al., 2009; Sinninghe Damsté et al., 2011). In the central Amazon Basin the branched GDGTs were mainly originated from erosion of lowland soils but a relatively small *in-situ* derived contribution in rivers and floodplain lakes was also observed (Kim et al., 2012; Zell et al., 2013a,b). Accordingly, the application of the BIT index based on the relative abundance of branched GDGTs versus crenarchaeol (Hopmans et al., 2004) appears to be useful to trace soil OM in the central Amazon Basin (cf. Kim et al., 2012). The GDGT-based proxies thus helped us to understand how the OM sources in the floodplain lakes were changed according to the paleoclimatic and paleohydrological variations during the Holocene.

5.1. Santa Ninha and Maracá Lakes: directly and permanently connected to the Amazon River

The impact of the paleohydrological variations of the Amazon River was similar in the floodplain lakes which had direct and permanent connection with the Amazon River during the high and low water phases. During the Early and Middle Holocene, a reduced Amazon River inflow into floodplain lakes, with reduced water levels of the Amazon River, was evident in the two sedimentary records. In Maracá Lake, a gap in sedimentation occurred between 13,100 and 3,600 cal years BP (Moreira et al., 2013b) suggests that the lake dried up. This hiatus was most probably a consequence of a reduced discharge of the Amazon River which was caused by the weakened flooding in the western Amazon Basin (Moreira et al., 2012, 2013b). In Santa Ninha Lake between 5,600 and 5,000 cal years BP and in Maracá Lake between 3,600 and 2,700 cal years BP, the smectite contents were low (Fig. 5). Low amounts of smectite during the Middle Holocene suggest a reduced Amazon River influence on floodplain lakes. In Maraca Lake, the reduced Amazon River inflow was evidenced by a gap in sedimentation between 13,100 and 3,200 cal years BP (Moreira et al., 2013b).

During this period, in Santa Ninha Lake between 5,700 and 5,000 cal years BP and in Maracá Lake between 3,600 and 2,700 cal years BP, the reduced river inflow was associated with high levels of TOC contents. This suggests that the lake water bodies were shallow which prevented from the dilution of TOC with the river transported lithogenic compounds (Fig. 5). The diminished availability of oxygen in shallow water lakes can improve the preservation of the OM (Meyers, 1993) and thus, high levels of TOC were recorded in Santa Ninha and Maracá Lakes during periods with low river inflow. The OM preservation is strongly dependent on the oxygen exposure since the anaerobic organisms presented in an anoxic environment are less efficient degraders of OM than aerobic organisms (Zonneveld et al., 2010). As observed by Moreira et al. (2012) in Santa Ninha Lake, during this phase the microscopic analyses revealed the presence of cuticles and well-preserved tissues that support an enhanced OM preservation due to anoxic conditions. Such environment might correspond to a marsh with low litho-clastic input (Turcq et al., 2002) and the local moisture was maintained by the water supply from the local watershed, as suggested by the high kaolinite contents during this period. During the periods of reduced Amazon River input into the floodplain lakes, high branched GDGT concentrations were recorded in Santa Ninha and Maracá Lakes (Fig. 5). The BIT values were similar in both lakes and close to the average value of Amazon soils (0.97, Kim et al., 2012; Zell et al., 2013a,b) which supports a predominant sedimentary supply from the watershed.

An increase in the Amazon River influence during the Late Holocene was indicated by the increase in smectite concentration in Santa Ninha Lake after 5,000 cal years BP (Moreira et al., 2012) and in Maracá Lake after 2,700 cal years BP (Moreira et al., 2013b), as represented by the Fig. 5. A transition to a humid condition during Late Holocene was marked by a drastic decrease in TOC contents in Santa Ninha and Maracá Lakes (Moreira et al., 2012, 2013b) and highlighted the contribution of litho-clastic input that diluted the sedimentary OM produced in the lacustrine environments (Turcq et al., 2002). During the periods of high fluvial inflows into the floodplain lakes, although branched GDGTs were still predominant, crenarchaeol proportions to the sedimentary GDGT pool increased, as observed by the decreases in BIT values after 5,000 cal years BP in Santa Ninha Lake and after 2,700 cal years BP in Maracá Lake (Fig. 5). This suggests that aquatic-produced crenarchaeol contributions increased during the Late Holocene in comparison to during the Early and Middle Holocene.

During the Late Holocene, a sharp contact was observed in TA14 core (34 cm) and in MAR2 core (35.5 cm and 55.5 cm). This may correspond to a break in sedimentation, which can be interpreted as a consequence of a strong erosive event. Therefore, longer periods of high water levels of the Amazon River or catastrophic flood events probably had a strong influence on these floodplain lakes (Moreira et al., 2012).

5.2. Comprido Lake: indirectly connected to the Amazon River

Comprido Lake is an isolated lake that is indirectly connected to the Amazon River through Maraca Lake (Moreira et al., 2013a). The sediment supply in this lake primarily originates from the local drainage basin with modest contribution from the flooding of the Amazon River (Moreira et al., 2013a). The predominance of kaolinite along the Comprido Lake record confirms that the supply from the local watershed dominates in this lake (Fig. 5). This difference, in comparison with Santa Ninha and Maraca Lakes, results in a contrasting response to the variations in the paleohydrology of the Amazon Basin.

In Comprido Lake, the weakened connection with the Amazon River was recorded between 10,300 and 3,000 cal years BP. A dry climatic condition between 10,300 and 7,800 cal years BP was suggested by an increase in the abundance of C_4 grasses on unflooded mud banks followed by a gap in sedimentation due to a complete dryness of the lake between 7,800 and 3,000 cal years BP. However, the mineralogical composition showed no variation in the COM1 record, with kaolinite as the main clay mineral (Fig. 5). This mineralogical composition indicates the predominant terrestrial input by the surface runoff from the local catchment area (Moreira et al., 2013a).

During the dry period, low TOC contents were recorded in Comprido Lake, in contrast with the preservation of the OM occurred in Santa Ninha and Maracá Lakes.

The different impact on TOC contents observed in the studied lakes during the periods with lower fluvial inflows might be attributed to the connection with the Amazon River main stem. Due to the indirect connection with the main channel the low Amazon River water phase should have a more drastic impact on Comprido Lake. Therefore, the periods of low river input might have caused the dryness of the lake. The low TOC values can be due to the low OM sedimentation or can be a consequence of the enhanced degradation due to the increased exposure time to oxygen on open unflooded mud areas, characteristic of prolonged dry phases. Huguet et al (2009) observed a substantial degradation of GDGTs in oxidized regions of turbidites when compared to unoxidized parts. Hence, the reduced concentrations of crenarchaeol and branched GDGTs (see Fig. 5) might be due to a partial degradation of these compounds as a result of long term exposure to oxic conditions due to low lake water levels.

Although the direct river influence on Comprido Lake was difficult to constrain, there was a clear increase in humidity around the lake during the Late Holocene. The transition to the humid phase in Comprido Lake was characterized by the increase in TOC content, in contrast with the dilution of TOC observed in Santa Ninha and Maracá Lakes. This difference can be also attributed to the distance of Comprido Lake from the Amazon River main channel. Since this lake is indirectly connected to the Amazon River the litho-clastic input was reduced and consequently the sedimentary OM was not diluted by the fluvial inflow, as can be attested by the predominance of kaolinite and low smectite content during all the record (Fig. 5). In addition a gradual increase of chlorophyll derivatives and *Aulacoseira* sp. during the Late Holocene suggest an increase in lake productivity and in lake water level due to more humid conditions (Moreira et al., 2013a). The chlorophyll derivatives described by Moreira et al (2013a) represents the chlorophyll degradation products extracted from sediments with 90 %

acetone which are collectively defined as sedimentary chlorophyll, according to Vallentyne (1955). The increasing abundance of planktonic species, like *Aulacoseira* sp., and chlorophyll derivatives reflects the expansion of water bodies, higher water levels and consequently increased effective moisture in the watershed (Servant and Servant-Vildary, 2003; Moreira et al., 2013a).

5.3. Paleohydrological impacts on bulk sedimentary OM sources

The C:N atomic ratios and $\delta^{13}C_{TOC}$ were used as indicator for the source of the sedimentary OM (Fig. 6). As observed in TA14 core, extremely low TOC contents were also recorded in the lowermost section of COM1 core (Fig. ,5) and the OM source in these cases must also be interpreted with caution. In sediments with low TOC contents (<0.3 wt. %), the relative proportion of inorganic nitrogen can be large and, consequently it yields C:N atomic ratios artificially depressed (Meyers, 1997; Meyers and Teranes, 2001). The samples with low TOC values were therefore excluded in Fig. 6.

The boundaries of the major source of OM presented in Fig. 6 were based on previous studies in the Amazon Basin, adapted from Kim et al. (2012) and references therein. In short, the C_3 plants in the Amazonian forests show a $\delta^{13}C_{TOC}$ value of -27 to -35 ‰ and a C:N atomic ratio of 13-330 (Hedges et al., 1986; Martinelli et al., 1994, 2003). The $\delta^{13}C_{TOC}$ of C_4 plants varies between -9 and -16 ‰ and the C:N atomic ratio is about 14-48 (Martinelli et al., 2003; Moreira-Turcq et al., 2013). Phytoplankton and periphyton in the Amazon aquatic systems typically have low $\delta^{13}C_{TOC}$ values (-28 to -34 ‰) according to Araújo-Lima et al. (1986) but localised phytoplankton blooms in floodplain lakes can have enriched carbon isotopic composition with the maximum of -23 ‰ (Moreira-Turcq et al., 2013).

The periods of low Amazon River influence in Santa Ninha and Maracá Lakes were characterized by predominant OM with a C_3 plant origin that may correspond to a floodplain forest (Igapó forest) or to a macrophyte bank. Although the OM source in COM1 core during the period of reduced Amazon River input were not shown in Fig. 6 due to the low TOC contents, the enriched carbon isotopic composition suggests the occurrence of C_4 plants during that period, as described by Moreira et al. (2013b). The enriched values of $\delta^{13}C_{TOC}$ observed between 10,300 and 7,800 cal years BP in Comprido Lake were associated with low values of TOC and chlorophyll derivatives, suggesting the development of a C_4 grasses (*graminea*) on unflooded areas due to prolonged periods of low water levels (Moreira et al., 2013b).

The differences of the OM sources between the periods of low and high water levels were apparent in Santa Ninha and Maracá Lakes (Fig. 6). Increased inputs of the Amazon River water into the floodplain lakes led to favorable conditions for aquatic primary production, reflected by lower C:N atomic ratios in these lakes. In Maracá Lake, the increased inflow of the Amazon River after 2,700 cal years BP was accompanied by an increase in the $\delta^{13}C_{TOC}$ values. This was interpreted as a higher input of C_4 macrophyte which marked the increased fluvial input into this lake (Moreira et al., 2013b). The floodplains associated with large rivers presents high levels of inorganic nutrients transported by the rivers and thus, high productive levels (Piedade et al., 2010). Some of the C_4 semi-aquatic and aquatic grasses (such as *P. fasciculatum* and E. *polystachia*, respectively) require high levels of nutrients (Piedade et al., 2010), which may thus explain the high $\delta^{13}C_{TOC}$ values accompanied by an increased fluvial input into Maracá Lake. However, during the period of a higher fluvial input, an increased contribution of phytoplankton was also detected in the Maraca Lake. On the other hand, the predominance of C_3-derived OM during the same period as the main source in Comprido Lake indicated that this lake received a large proportion of land-derived OM from the local catchment area.

5.4. Paleohydrological changes revealed by the GDGT distribution

Crenarchaeol and branched GDGTs were found in all three lake sediment cores at varying concentrations through time (Fig. 5). The presence of both crenarchaeol and branched GDGTs in the studied lakes is consistent with their presence in the high Andes and lowland Amazon soils (Weijers et al., 2006; Bendle et al., 2010; Huguet et al., 2010; Kim et al., 2012; Zell et al., 2013a) as well as in suspended particulate matter of Amazonian rivers and floodplain lakes in the central Amazon Basin (Zell et al., 2013a,b). In general, the MBT values (representing the degree of methyl branching) were high while the DC values (representing the number of cyclopentane moieties) were low in all the three records (Fig. 8). These distribution patterns were thus similar to those of lowland Amazon soils, but distinctive from those of high Andean soils (Fig. 8A). Accordingly, the MBT/CBT-derived MAAT of lake sediment cores was much closer to that of lowland Amazon soils rather than high Andean soils (Fig. 8B). Previously, Kim et al. (2012) showed that branched GDGTs in the suspended particulate matter of Amazonian rivers did not predominantly originate from high Andes soils (>2500 m in altitude). Hence, our results are in a good agreement with the previous finding that the high mountainous Andes are not a major source of branched GDGTs in the Amazon River (Kim et al., 2012). Taken together, the sedimentary branched GDGTs in Santa Ninha, Maracá, and Comprido Lakes were primarily derived from lowland Amazon soils.

During the Late Holocene, the increased contribution of crenarchaeol linked to higher lake water levels lowered the BIT index (Fig. 5), suggesting an increase in aquatic-produced crenarchaeol in Santa Ninha and Maracá Lakes. This is consistent with recent studies conducted in the central Amazon Basin (Kim et al., 2012; Zell et al., 2013a,b) which showed that crenarchaeol is indeed being produced *in-situ* in rivers as well as in floodplain lakes and results in decreased BIT values in comparison to those of lowland Amazon soils. During the same period, the MBT values decreased while the DC values increased in comparison to during the Early and Middle Holocene (Fig. 5). Consequently, the reconstructed pH values were generally higher than those from the Early and Middle Holocene whilst the MBT/CBT-derived MAAT remained in a similar range. Interestingly, these distributions of branched GDGTs (Fig. 8) were also quite different from those of lowland Amazon soils, i.e. the fractional abundances of branched GDGT Ib and IIb were substantially higher in Santa Ninha Lake as previously observed in Maracá Lake (Moreira et al., 2013b). The lowland Amazon soil types of the studied sites are classified as ferralsol and acrisol characterized by low soil pH (Quesada et al., 2009). This indicates that the branched GDGTs deposited in both Santa Ninha and Maracá Lakes during the Late Holocene did not predominantly originate from acidic soils transported from the surrounding terra firme through local black water streams, known locally as igarapés. Accordingly, there was an apparent shift in the source of branched GDGTs from the Early and Middle Holocene to the Late Holocene corresponding to a change in the hydrological regime. Moreira et al. (2013b) previously speculated that a major part of the branched GDGTs in the Maracá Lake during the Late Holocene might be transported by the Amazon River containing branched GDGTs originating from high Andean soils with higher soil pH. Similarly, the Santa Ninha Lake might have received more Andean-originated branched GDGTs during the same period. This hypothesis is seemingly supported by the enhanced proportion of Andean-derived smectite in both Santa Ninha and Maracá Lakes during the Late Holocene (Fig. 5).

However, the distributions of branched GDGTs of the Late Holocene lake sediments were different from those of the high Andean soils which have roughly equal amounts of branched GDGT Ia and IIa, and thus low MBT values (Fig. 8). Hence, it appears that branched GDGTs deposited in Santa Ninha and Maracá Lakes during the Late Holocene did not predominantly originate from high Andes soils, and thus the major sources of sediment and branched GDGTs were different during that period. However, we cannot exclude that they might have the sources of the lower montane forest vegetation belt (500–2500 m in altitude) in the Andes. It should be noted that branched GDGTs are also being produced *in-situ* in floodplain lakes and in rivers in the central Amazon Basin (Zell et al., 2013a,b). Hence, alternatively, the aquatic production in rivers might have been at least partly responsible for changing the branched GDGT distribution during the Late Holocene. However, the distribution of branched GDGTs of Santa Ninha and Maracá Lake sediments during the Late Holocene was different from those of the Amazon River suspended particulate matter (SPM) as well, with a higher DC but similar MBT range (Fig. 8). As a result, reconstructed pH and MAAT were higher than those of the Amazon River SPM. This suggests that the distribution of the *in-situ* produced branched GDGTs in floodplain lakes might be different in comparison to that in rivers, although the reasons are yet unknown.

In Comprido Lake, the concentrations of branched GDGTs were much higher during the Late Holocene than during the Early and Middle Holocene (Fig. 5). However, the BIT values remained high through time. The MBT and the DC were different in comparison to those from Santa Ninha and Maracá Lakes during the same period (Fig. 8). In Comprido Lake, the MBT and DC values were much closer to those of the lowland Amazon soils and deviated from those of high Andean soils and the Amazon River SPM (Fig. 8). This suggests that in comparison to Santa Ninha and

Maracá Lakes, Comprido Lake had an increased supply of branched GDGTs from the local catchment area than by the Amazon River or by the *in-situ* production in the lake itself. This hypothesis can be supported by higher proportion of lowland-derived kaolinite than Andean-derived smectite during the entire Holocene (Fig. 5).

5.5. Comparison with other Amazonian paleoclimatic records

The evidences of low influence of the Amazon River on the floodplain lakes in our study sites during the Early and Middle Holocene are in agreement with periods of generally drier climatic conditions recorded in different locations around the Amazonian Basin. During the Early and Middle Holocene, charcoal depositions increased in lakes and soils, savannas were expanded, and lake water levels lowered. These evidences come from various parts of the Amazon Basin based on a large number of multi-proxy lake sediment and soil studies: Northern Amazonia (Saldarriaga and West, 1986; Desjardins et al., 1996; Behling and Hoogmiestra, 1999; Turcq et al., 2002), Central Amazonia (Absy, 1979; Soubies, 1979; Behling et al., 2001), Southern and South-western Amazonia (Mayle et al. 2000; De Freitas et al. 2001), Eastern Amazonia (Sifeddine et al. 1994, 1998, 2001; Cordeiro et al., 1997, 2008; Turcq et al. 1998; Irion et al., 2006; Bush et al., 2007; Moreira et al., 2012, 2013a,b), Western Amazonia (Weng et al. 2002,), and Andian regions (Baker et al. 2001; Weng et al. 2006; Hillyer et al. 2009). The Early and Middle Holocene dry period was attributed to the weakened monsoon due to a lower summer insolation in the Southern Hemisphere during that period, which replaced the inter tropical convergence zone (ITCZ) more northwards than the Present.

Multiple lines of evidences such as the increased amount of smectite, the dilution of TOC, the increased contribution of phytoplankton to the buried OM combined with higher DC and lower MBT values in our study sites indicate higher fluvial input associated with higher Amazon River levels during the Late Holocene. This, in turn suggests a more humid phase during the Late Holocene. A shift to a wetter condition towards the Late Holocene was also recorded in several lowland Amazonian sites (Behling and Hooghiemstra, 1999; Behling and Costa, 2000; Behling et al., 2001; Cordeiro et al., 2008). For example, Behling et al. (2001) observed a decrease in TOC accompanied by a decrease of Poacea pollen and increased proportion of várzea/igapo forests in Calado Lake, located in the central Amazon Basin, since 2,080 ^{14}C year BP. These authors interpreted these records as an evidence of a longer high-stand of water levels of the Amazon River. In the central Amazon Basin, a decrease in the frequency of drought events since 4,200 cal years BP was also observed in Tapajos Lake by Irion et al. (2006). The last millennium was considered to be the period of highest sustained lake water levels over the Amazon Basin (Bush et al., 2007).

Although the Santa Ninha, Maracá and Comprido Lake records showed a consistent, overall pattern of wetter climatic conditions from the Early and Middle to Late Holocene, which was consistent with the general hydro-climatic evolution over the Amazon Basin, some discrepancies were also observed during the transitional period from a drier to a wetter condition among the three lake records. Our records showed about a 2,000-year lag in the timing of the increase in the Amazon River inflow between the floodplain lakes. The river inflow was substantially higher in Santa Ninha Lake after 5,000 cal years BP, while in Maraca and Comprido Lakes, higher river inflows started at 2,700 and 3,000cal years BP, respectively. A longer dry phase was thus observed in Maracá and Comprido Lakes reflected by extremely low values of TOC followed by a break in sedimentation during the Early and Middle Holocene (Moreira et al., 2013a,b). However it should be noted that during this period, although evidences of lower lake water levels in Santa Ninha Lake was recorded, some influences of the Amazon River were still detected by the presence of smectite in this lake (Fig. 5). These results suggest that Maraca and Comprido Lakes, during the Early-Middle Holocene, were more isolated from the Amazon River than Santa Ninha Lake. During the Late Holocene, Santa Ninha Lake also presented evidences of more fluvial influence than in the other lakes with highest crenarchaeol concentration and lowest BIT index. Hence, the 2,000-year time lag seems to be a consequence of differences in the connection and distance of the lakes to the Amazon River main channel. Nowadays, the heterogeneous, seasonal patterns in precipitation across the Amazon Basin (Mayle and Power, 2008) and the size and complexity of the Amazon floodplain lakes (Melack and Forsberg, 2001) are subjected to oscillations in inflow of the Amazon River and its tributaries (Richey et al. 1989). Similarly, a complex Amazon River system during the Holocene might also be responsible for the differences in the timing of the transition from a drier to a wetter condition among the floodplain lakes.

6. CONCLUSIONS

The sources and the depositional processes of the sedimentary OM in Santa Ninha, Maracá, and Comprido Lakes, which are located in the central Amazon Basin and have different characteristics in terms of the lake size and the connectivity to the Amazon River main stem, were investigated in this study. The mineralogical and organic geochemical parameters used were clay mineralogy, TOC content, C:N atomic ratio, $\delta^{13}C_{TOC}$, and GDGT concentrations and indices. The Early and Middle Holocene was characterized by a reduced inflow of the Amazon River into the floodplain lakes, as indicated by the low Andean-derived smectite content. It appears that the reduced Amazon River floods during this period caused high TOC accumulations in Santa

Ninha and Maracá Lakes due to a reduced dilution by lithogenic compounds transported by the Amazon River. At the same time, sedimentary OM was predominantly derived from C_3 plants and was associated with acid soil OM transported by local black water streams (igarapés) to the lakes. The increase in the Amazon River influence during the Late Holocene was revealed by higher Andean-derived smectite content at the expense of lowland-derived kaolinite. During this period, the TOC contents decreased due to the enhanced dilution by lithogenic compounds and the contribution of aquatic-produced OM to sedimentary OM pool was increased in Santa Ninha and Maracá Lakes. The impact of hydrological variations in the Amazon River on Comprido Lake was different since this lake was connected to Maracá Lake and thus indirectly influenced by the Amazon River. In contrast to the Santa Ninha and Maracá Lakes, the TOC contents increased during the Late Holocene due to the better preservation of the soil OM associated with the increased lake water level. This was attested by the predominance of lowland-derived kaolinite. The sedimentary OM in Comprido Lake was characterized by C_3-derived plants mainly delivered from acidic soils of the local catchment area rather than by the Amazon River. Accordingly, this study showed that the Amazon River hydrological changes controlled the sources and the depositional processes of sedimentary OM in the floodplain lakes in different ways depending on how the lakes were connected to the Amazon River main stem.

Acknowledgements

This research was supported by the French Research Institute for the Development (IRD), by the HYBAM Research Program (Hydrology and Geochemistry of the Amazonian Basin, www.mpl.ird.fr/hybam/) in the frame of its cooperation agreement with the Brazilian Research Centre (CNPq process nos. 492685/2004–05 and

690139/2003–09). This project was also supported by the project INSU Paleo2 – PASCAL (Past climate change impacts on carbon accumulation in Amazonia floodplain lakes (2010-2012)) and by the French project ANR ELPASO 2010 BLANC 608-01. L. Moreira's work was supported by a fellowship of CNPq, Brazil. The research leading to these results has also received funding from the European Research Council under the European Union's Seventh Framework Programme (FP7/2007-2013) / ERC grant agreement n° [226600]. The authors would like to thank the technical groups of Agência Nacional das Águas from Brazil (ANA) and Companhia de Pesquisa dos Recursos Minerais (CPRM, Manaus) for their help during the cruise as well as J. Ossebaar at NIOZ for analytical support. We are also very grateful to P. A. Meyers and two anonymous reviewers for their constructive comments which substantially improved the manuscript.

REFERENCES

Abbott, M. B., Wolfe, B. B., Wolfe, A. P., Seltzer, G. O., Aravena, R., Mark, B. G., Polissar, P. J., Rodbell, D. T., Rowe, H. D., Vuille, M., 2003. Holocene paleohydrology and glacial history of the central Andes using multiproxy lake sediment studies. Palaeogeography, Palaeoclimatology, Palaeoecology 194, 123–138.

Absy, M. L., 1979. A Palynological study of Holocene sediments in the Amazon Basin. Ph.D. thesis, University of Amsterdam, Netherlands.

Amorim, M. A., 2010. Sedimentação e acúmulo de carbono durante o Holoceno em um sistema de várzeas da Amazônia: Várzea do Lago Grande do Curuai, Pará, Brasil. Ph.D. thesis. Universidade Federal Fluminense, Niterói, Brazil.

Araújo-Lima, C. A. R. M., Forsberg, B. R., Victoria, R., Martinelli, L., 1986. Energy sources for detritivorous fishes in the Amazon. Science 234, 1256–1258.

Baker, P. A., Seltzer, G. O., Fritz, S. C., Dunbar, R. B., Grove, M. J., Tapia, P. M., Cross, S. L., Rowe, H. D., Broda, J. P., 2001. The history of South American tropical precipitation for the past 25,000 years. Science 291, 640–643.

Behling, H., Keim, G., Irion, G., Junk, W., De Mello, J., 2001. Holocene environmental changes in the Central Amazon Basin inferred from Lago Calado (Brazil). Palaeogeography, Palaeoclimatology, Palaeoecology 173, 87–101.

Behling, H., Costa, L. D, 2000. Holocene environmental changes from the Rio Curuá record in the Caxiuana Region, Eastern Amazon Basin. Quaternary Research 53, 369–377.

Behling, H., Hooghiemstra, H., 1999. Late Quaternary palaeoecology and palaeoclimatology from pollen records of the savannas of the Llanos Orientales in Colombia. Palaeogeography, Palaeoclimatology, Palaeoecology 139, 251–267.

Bendle, J. A., Weijers, J. W. H., Maslin, M. A., Sinninghe Damsté, J. S., Schouten, S., Hopmans, E. C., Boot, C. S., Pancost, R. D, 2010. Major changes in glacial and Holocene terrestrial temperatures and sources of organic carbon recorded in the Amazon fan by tetraether lipids. Geochemistry Geophysics Geosystems 11, Q12007, doi:10.1029/2010GC003308.

Blaauw, M., Christen, J.A., 2011. Flexible paleoclimate age-depth models using an autoregressive gamma process. Bayesian Analysis 6, 457–474.

Bush, M. B., Silman, M. R., Listopad, C. M. C. S., 2007. A regional study of Holocene climate change and human occupation in Peruvian Amazonia. Journal of Biogeography 34, 1342–1356.

Cordeiro, R. C., Turcq, B., Oliveira Da Silva, A., Suguio, K., 1997. Holocene environmental changes in Carajás region (Pará, Brazil) recorded by lacustrine deposits. Proceedings of the International Association of Theoretical and Applied Limnology 26, 814–817.

Cordeiro, R. C., Turcq, B., Suguio, K., Silva, A. O., Sifeddine, A., Volkmer-Ribeiro, C., 2008. Holocene fires in east Amazonia (Carajás), new evidences, chronology and relation with paleoclimate. Global and Planetary Change 61, 49–62.

De Freitas, H. A., Pessenda, L. C. R., Aravena, R., Gouveia, S. E. M., Ribeiro, A. S., Boulet, R., 2001. Late Quaternary vegetation dynamics in the Southern Amazon Basin inferred from carbon isotopes in soil organic matter. Quaternary Research 55, 39–46.

De Toledo, M. B., Bush, M. B., 2008. Vegetation and hydrology in Eastern Amazonia inferred from a pollen record. Anais da Academia Brasileira de Ciencias 80, 191-203.

Desjardins, T., Carneiro-Filho, A., Mariotti, A., 1996. Changes of the forest-savanna boundary in Brazilian Amazonia during the Holocene revealed by stable isotope ratios of soil organic carbon. Oecologia 108, 749–756.

Dias, P. L. S., Turcq, B., Dias, M. A. F. S., Braconnot, P., Jorgetti, T., 2009. Mid-Holocene climate of tropical South America: a model-data approach. In: Past Climate Variability in South America and Surrounding Regions. Developments in Paleoenvironmental Research 14, 259-281.

Dunne, T., Mertes, L. A. K., Meade, R. H., Richey, J. E., Forsberg, B. R., 1998. Exchanges of sediment between the flood plain and the channel of the Amazon River in Brazil. Geological Society of America Bulletin 110, 450–467.

Guyot, J. L., Jouanneau, J. M., Soares, L., Boaventura, G. R., Maillet, N., Lugane, C., 2007. Clay mineral composition of river sediments in the Amazon Basin. Catena 71, 340–356.

Hedges, J. I., Clark, W. A., Quay, P. D., Richey, J. E., Devol, A., Santos, U., 1986. Composition and fluxes of particulate organic material in the Amazon River. Limnology and Oceanography 31, 717–738.

Hermanowski, B., Lima da Costa, M., Behling, H., 2012. Environmental changes in southeastern Amazonia during the last 25,000 yr revealed from a paleoecological record. Quaternary Research 77, 138–148.

Hillyer, R., Valencia, B. G., Bush, M., Silman, M. R., Steinitz-Kannan, M. A., 2009. 24,700-yr paleolimnological history from the Peruvian Andes. Quaternary Research 71, 71–82.

Hogg, A. G., Hua, Q., Blackwell, P. G., Niu, M., Buck, C. E., Guilderson, T. P., Heaton, T. J., Palmer, J. G., Reimer, P. J., Reimer, R. W., Turney, C. S. M., Zimmerman. S. R. H., 2013. SHCAL13 southern hemisphere calibration, 0–50,000 years cal BP. Radiocarbon 55, 1889–1903.

Hopmans, E. C., Weijers, J. W. H., Schefuß, E., Herfort, L., Sinninghe Damsté, J. S., Schouten, S., 2004. A novel proxy for terrestrial organic matter in sediments based on branched and isoprenoidtetraether lipids. Earth and Planetary Science Letters, 224, 107–116.

Huguet, A., Fosse, C., Metzger, P., Fritsch, E., Derenne, S., 2010. Occurrence and distribution of extractable glycerol dialkyl glycerol tetraethers in podzols. Organic geochemistry 41, 291–301.

Huguet, C., Hopmans, E. C., Febo-Ayala, W., Thompson, D. H., Sinninghe Damsté, J. S., Schouten, S., 2006. An improved method to determine the absolute abundance of glycerol dibiphytanyl glycerol tetraether lipids. Organic Geochemistry 37, 1036–1041.

Irion, G., 1984. Clay minerals of Amazon soils. In: Sioli, H. (Ed.), The Amazon. Limnology and landscape of a mighty tropical river and its Basins (Monographiae Biologicae), Dordrecht, pp. 537–579.

Irion, G., Bush, M. B., Nunes De Mello, J. A., Stuben, D., Neumann, T., Muller, G., Morais, J. O., Junk, J. W., 2006. A multiproxy palaeoecological record of Holocene lake sediments from the Rio Tapajós, eastern Amazonia. Palaeogeography, Palaeoclimatology, Palaeoecology 240, 523–536.

Jones, P. D., Briffa, K. R., Osborn, T. J., Lough, J. M., Van Ommen, T. D., Vinther, B. M., Luterbacher, J., Wahl, E. R., Zwiers, F. W., Mann, M. E., Schmidt, G. A., Ammann, C. M., Buckley, B. M., Cobb, K. M., Esper, J., Goosse, H., Graham, N., Jansen, E., Kiefer, T., Kull, C., Küttel, M., Mosley-Thompson, E., Overpeck, J. T., Riedwyl, N., Schulz, M., Tudhope, A. W., Villalba, R., Wanner, H., Wolff, E., Xoplaki, E., 2009. High-resolution palaeoclimatology of the last millennium: a review of current status and future prospects. The Holocene 19, 3-49.

Kim, J.-H., Ludwig, W., Schouten, S., Kerherv, P., Herfort, L., Bonnin, J., Sinninghe Damsté, J. S., 2007. Impact of flood events on the transport of terrestrial organic matter to the ocean: A study of the Têt River (SW France) using the BIT index. Organic Geochemistry 38, 1593–1606.

Kim, J.-H., Zarzycka, B., Buscail, R., Peterse, F., Bonnin, J., Ludwig, W., Schouten, S., Sinninghe Damsté, J. S., 2010. Contribution of river-borne soil organic carbon to the Gulf of Lions (NW Mediterranean). Limnology and Oceanography 55, 507–518.

Kim, J.-H., Zell, C., Moreira-Turcq, P., Pérez, M. A. P., Abril, G., Mortillaro, J.-M., Weijers, J. W. H., Meziane, T., Sinninghe Damsté, J. S., 2012. Tracing soil organic carbon in the lower Amazon River and its tributaries. Geochimica et Cosmochimica Acta 90,163–180.

Latrubesse, E. M., Cozzuol, M., Silva-Caminha, S. A. F., Rigsby, C. A., Absy, M. L., Jaramillo, C., 2009. The Late Miocene paleogeography of the Amazon Basin and the evolution of the Amazon River system. Earth-Science Reviews 99, 99–124.

Martinelli, L. A., Victoria, R. L., Forsberg, B. R., Richey, J. E., 1994. Isotopic composition of major carbon reservoirs in the Amazon floodplain. International Journal of Ecology and Environmental Sciences 20, 31–46.

Martinelli, L. A., Victoria, R. L., de Camargo, P. B., Piccolo, M. C., Mertes, L., Richey, J. E., Devol, A. H., Forsberg, B. R., 2003. Inland variability of carbon–nitrogen concentrations and $\delta^{13}C$ in Amazon floodplain (várzea) vegetation and sediment. Hydrological Process 17, 1419–1430.

Martinez, J. M., Toan, T. L., 2007. Mapping of flood dynamics and spatial distribution of vegetation in the Amazon floodplain using multitemporal SAR data. Remote Sensing of Environment 108, 209–223.

Martins, G. S., Fontes D., Cordeiro, R. C., Turcq, B., Moreira, L. S., Rodrigues, R. A., Guilles, M. C. C., Santos, A. B., Sifeddine, A., Seoane, J. C. S., Barros, M. A., Barth, O. M., Behling, H., 2014. Environmental changes in the last 35 kyrs from the Saci Lake record, Pará state - southeastern Amazon Basin.

Mayle, F. E., Burbridge, R., Killeen,T. J., 2000. Millennial-Scale Dynamics of Southern Amazonian Rain Forests. Science 290, 2291–2294.

Mayle, F. E., Power, M. J., 2008. Impact of a drier Early-Mid-Holocene climate upon Amazonian forests. Philosophical Transactions of the Royal Society of London B Biological Sciences 363, 1829-1838.

Melack, J. M., Forsberg, B. R., 2001. Biogeochemistry of Amazon Floodplain Lakes and Associated Wetlands. In: McClain, M. E., Victoria, R. L., Richey, J. E (eds). The biogeochemistry of the Amazon basin. Oxford University Press, New York, NY, pp 235–274.

Mendes, A. C., Truckenbrod, W., Nogueira, A. C. R., 2012. Análise faciológica da Formação Alter do Chão (Cretáceo, Bacia do Amazonas), próximo à cidade de Óbidos, Pará, Brasil. Revista Brasileira de Geociências 42, 39-57.

Mertes, L. A. K., 1994. Rates of floodplain sedimentation on the central Amazon River. Geology 22, 171–174.

Meyers, P. A., 1993. Origin of the Plio-Pleistocene Vrica laminites" organic geochemical evidence. Marine Geology 115, 117-127.

Meyers, P. A., 1994. Preservation of elemental and isotopic source identification of sedimentary organic matter. Chemical Geology 114, 289–302.

Moreira, L. S., Moreira-Turcq, P., Turcq, B., Caquineau, S., Cordeiro, R .C., 2012. Paleohydrological changes in an Amazonian floodplain lake: Santa Ninha Lake. Journal of Paleolimnology 48, 339–350.

Moreira, L. S., Moreira-Turcq, P., Cordeiro, R. C., Turcq., B., Caquineau, S., Viana, J. C. C., Brandini, N., 2013a. Holocene paleoenvironmental reconstruction in the Eastern Amazonian Basin: Comprido Lake. Journal of South American Earth Science 44, 55–62.

Moreira, L. S., Moreira-Turcq, P., Turcq, B., Cordeiro, R. C., Kim, J.-H., Caquineau, S., Mandengo Yogo, M., Sinninghe Damsté, J. S., 2013b. Paleohydrological controls on sedimentary organic matter composition in an Amazon floodplain lake, Lake Maracá (Brazil) during the Late Holocene. The Holocene 23, 1903–1914.

Moreira-Turcq, P., Bonnet, M. P., Amorim, M., Bernardes, M., Lagane, C., Maurice, L., Perez, M., Seyler, P., 2013. Seasonal variability in concentration, composition, age, and fluxes of particulate organic carbon exchanged between the floodplain and Amazon River. Global Biogeochemical Cycles 27, 119–130.

Moreira-Turcq, P., Jouanneau, J. M., Turcq, B., Seyler, P., Weber, O., Guyot, J. L., 2004. Carbon sedimentation at Lago Grande de Curuai, a floodplain lake in the low Amazon region: insights into sedimentation rates. Palaeogeography, Palaeoclimatology, Palaeoecology 214, 27–40.

Nogueira, A., Sarges, R., 2001. Characterization and genesis of waterfalls of the Presidente Figueiredo region, northeast State of Amazonas, Brazil. Anais da Academia Brasileira de Ciências 73,

Pancost, R. D., Sinninghe Damsté, J. S., 2003. Carbon isotopic compositions of prokaryotic lipids as tracers of carbon cycling in diverse settings. Chemical Geology 195, 29–58.

Pearson, E. J., Juggins, S., Talbot, H. M., Weckström, J., Rosén, P., Ryves, D. B., Roberts, S. J., Schimidt, R., 2011. A lacustrine GDGT-temperature calibration from the Scandinavian Arctic to Antarctic: Renewed potential for the application of GDGT-paleothermometry in lakes. Geochimica et Cosmochimica Acta 75, 6225–6238.

Peterse, F., Nicol, G. W., Schouten, S., Sinninghe-Damsté, J. S., 2010. Influence of soil pH on the abundance and distribution of core and intact polar lipid-derived branched GDGTs in soil. Organic Geochemistry 41, 1171–1175.

Peterse, F., van der Meer, J., Schouten, S., Weijers, J. W. H., Fierer, N., Jackson, R. B., Kim, J.-H., and Sinninghe Damsté, J. S., 2012. Revised calibration of the MBT–CBT paleotemperature proxy based on branched tetraether membrane lipids in surface soils. Geochimica et Cosmochimica Acta 96, 215–229.

Piedade, M. T. F., Junk, W., D'Ângelo, S.A., Wittmann, F., Schöngart, J., Barbosa, K. M. N., Lopes, A., 2010. Aquatic herbaceous plants of the Amazon floodplains: state of the art and research needed. Acta Limnologica Brasiliensia 22, 165-178.

Pitcher, A., Hopmans, E. C., Mosier, A. C., Park, S.-J., Rhee, S.-K., Francis, C. A., Schouten, S., Sinninghe Damsté, J. S., 2011. Core and intact polar glycerol dibiphytanyl glycerol tetraether lipids of ammonia-oxidizing archaea enriched from marine and estuarine sediments. Applied and Environmental Microbiology 77, 3468–3477.

Quesada, C. A., Lloyd, J., Anderson, L. O., Fyllas, N. M., Schwarz, M., Czimczik, C. I., 2011. Soils of Amazonia with particular reference to the RAINFOR sites. Biogeosciences 8, 1415–1440.

Radambrasil, folha SA.21 Santarém, 1974. Levantamento de Recursos naturais.

Richey, J. R., Hedges, J. I., Devol, A. H., Quay, P. D., Victoria, R., Martinelli, L. A., Forsberg, B. R., 1989. Biogeochemistry of carbon in the Amazon River. Limnology and Oceanography 35, 352–371.

Saldarriaga, J., West, D. C., 1986. Holocene fires in the northern Amazon Basin. Quaternary Research 26, 358–366.

Schouten, S., Hopmans, E. C., Schefuß, E., Sinninghe Damsté, J. S., 2002. Distributional variations in marine crenarchaeotal membrane lipids: a new tool for reconstructing ancient sea water temperatures? Earth Planetary Science Letters 204, 265–274.

Schouten, S., Middelburg, J. J., Hopmans, E. C., Sinninghe Damsté, J. S., 2010. Fossilization and degradation of intact polar lipids in deep subsurface sediments: a theoretical approach. Geochimica et Cosmochimica Acta 74, 3806–3814.

Servant, M., Servant-Vildary, M., 2003. Holocene precipitation and atmospheric changes inferred from river paleowetlands in the Bolivian Andes. Palaeogeography, Palaeoclimatology, Palaeoecology 194, 187-206.

Sifeddine, A., Fröhlich, F., Fournier, M., Martin, L., Servant, M., Soubiés, F., Suguio, K., Turcq, B., 1994. La sédimentation lacustre indicateur de changements des paléoenvironnements au cous des 30000 dernières annèes (Carajas, Amazonie, Brésil). Comptes rendus de l'Académie des sciences 318, 1645–1652 (in French, with English Abstr.).

Sifeddine, A., Martin, L., Turcq, B., Ribeiro, C. V., Soubiès, F., Cordeiro, R. C., Suguio, K., 2001. Variations of the Amazonian rainforest environment: A sedimentological record covering 30,000 years. Palaeogeography, Palaeoclimatology, Palaeoecology 168, 221–235.

Simões Filho, F. F. L., 2000. Sedimentação lacustre e implicações paleoambientais na região de contato floresta-savana de Roraima durante o Holoceno. Ph.D. thesis. Universidade Federal Fluminense, Niterói, Brasil.

Sinninghe Damsté, J. S., Hopmans, E. C., Pancost, R. D., Schouten, S., Geenevasen, J. A. J., 2000. Newly discovered non-isoprenoid glycerol dialkyl glycerol tetraether lipids in sediments. Chemical Communications 1683–1684.

Sinninghe Damsté, J. S., Hopmans, E. C., Schouten, S., Van Duin, A. C. T., Geenevasen, J. A. J., 2002. Crenarchaeol: the characteristic core glycerol dibiphytanyl glycerol tetraether membrane lipid of cosmopolitan pelagic crenachaeota. Journal of Lipid Research 43, 1641–1651.

Sinninghe Damsté, J. S., Ossebaar, J., Abbas, B., Schouten, S., Verschuren, D., 2009. Fluxes and distribution of tetraether lipids in an equatorial African lake: Constraints on the application of the TEX_{86} palaeothermometer and BIT index in lacustrine settings. Geochimica et Cosmochimica Acta 73, 4232–4249.

Sinninghe Damsté, J. S., Rijpstra, W. I. C., Hopmans, E. C., Weijers J. W. H., Foesel, B. U., Overmann, J., Dedysh, S. N., 2011. 13,16-Dimethyl Octacosanedioic Acid (iso-Diabolic Acid), a common membrane-spanning lipid of Acidobacteria subdivisions 1 and 3. Applied and Environmental Microbiology 77, 4147–4154.

Soubies, F., 1980. Existence d'une phase sèche en Amazonie brésilienne datée par la présence de charbons de bois (6000-3000 ans ANOS A.P.). ORSTOM, Série Géologique 1, 133-148 (in French, with English Abstr.).

Spang, A, Hatzenpichler, R., Brochier-Armanet, C., Rattei, T., Tischler, P., Spieck, E., Streit, W., Stahl, D. A., Wagner, M., Schleper, C., 2010. Distinct gene set in two different lineages of ammoniaoxidizing archaea supports the phylum Thaumarchaeota. Trends in Microbiology 18, 331-340.

Stuiver, M., Reimer, P. J., Bard, E., Beck, J.W., Burr, G. S., Hughen, K. A., Kromer, B., McCormac, F. G., v. d. Plicht, J., Spurk, M.,1998. INTCAL98 Radiocarbon age calibration 24,000 - 0 cal BP. Radiocarbon 40:1041–1083.

Turcq, B., Sifeddine, A., Martin, L., Absy, M. A., Soubies, F., Suguio, K., Volkmer-Ribeiro, C., 1998. Amazonia Rainforest fires: a lacustrine record of 7000 years. Ambio 27, 139–142.

Turcq, B., Albuquerque, A. L. S., Cordeiro, R.C., Sifeddine, A., Simões Filho, F. F. L., Souza, A.G., Abrão, J. J., Oliveira, F. B. L., Silva, A. O., Capitaneo, J., 2002. Accumulation of organic carbon in Five Brazilian lakes during the Holocene. Sedimentary Geology 148, 319–342.

Vallentyne, J. R, 1955. Sedimentary chlorophyll determination as a paleobotanical method. Canadian Journal of Botany 33, 304-313.

Volkoff, B., Cerri, C. C., 1987. Carbon isotopic fractionation in subtropical Brazilian grassland soils: Comparison with tropical forest soils. Plant and Soil 102, 27–31.

Weijers, J. W. H., Schouten, S., Van Den Linden, M., Van Geel, B., Sinninghe Damsté, J. S., 2004. Water table related variations in the abundance of intact archaeal membrane lipids in a Swedish peat bog. FEMS Microbiology Letters 239, 51–56.

Weijers, J. W. H., Schouten, S., Spaargaren, O. C., Sinninghe Damsté, J. S., 2006. Occurrence and distribution of tetraether membrane lipids in soils: Implications for the use of the TEX_{86} proxy and the BIT index. Organic Geochemistry 37, 1680–1693.

Weijers, J. W. H., Schouten, S., Van den Donker, J. C., Hopmans, E. C., Sinninghe Damsté, J. S., 2007. Environmental controls on bacterial tetraether membrane lipid distribution in soils. Geochimica et Cosmochimica Acta 71, 703-713.

Weijers, J. W. H., Wiesenberg, G. L. B., Bol, R., Hopmans, E. C., Pancost, R. D., 2010. Carbon isotopic composition of branched tetraether membrane lipids in soils suggest a rapid turnover and a heterotrophic life style of their source organism(s). Biogeosciences 7, 2959–2973.

Weng, C., Bush, M. B., Curtis, J. H., Kolata, A. L., Dillehay, T. D., Binford, M. W., 2006. Deglaciation and Holocene climate change in the western Peruvian Andes. Quaternary Research 66, 87–96.

Weng, C., Bush, M. B., Athens, J. S., 2002. Two histories of climate change and hydrarch succession in Ecuadorian Amazonia. Review of Palynology and Paleobotany 120, 73–90.

Zell, C., Kim, J.-H., Moreira-Turcq, P., Abril, G., Hopmans, E. C., Bonnet, M.-P., Lima Sobrinho, R., Sinninghe Damsté, J. S., 2013a. Disentangling the origins of branched tetraether lipids and crenarchaeol in the lower Amazon River: Implications for GDGT-based proxies. Limnology and Oceanography 58, 343–353.

Zell, C., Kim, J.-H., Abril, G., Sobrinho, R. L., Dorhout, D., Moreira-Turcq, P., Sinninghe Damsté, J. S. (2013b). Impact of seasonal hydrological variation on the distributions of tetraether lipids along the Amazon River in the central Amazon basin: implications for the MBT/CBT paleothermometer and the BIT index. Frontiers in Microbiology 4, doi: 10.3389/fmicb.2013.00228.

Zonneveld, K. A. F., Versteegh, G. J. M., Kasten, S., Eglinton, T. I., Emeis, K.-C., Huguet, C., Koch, B. P., de Lange, G. J., de Leeuw, J. W., Middelburg, J. J., Mollenhauer, G., Prahl, F. G., Rethemeyer, J., Wakeham, S. G., 2010. Selective preservation of organic matter in marine environments; processes and impact on the sedimentary record. Biogeosciences 7, 483–511.

Table legend

Table 1. The summary of AMS ^{14}C data of the sediment cores investigated according to Moreira et al. (2012, 2013a,b). Note that the AMS ^{14}C data were newly calibrated using the calibration curve of SHcal13 (Hogg et al., 2013).

Figure captions

Fig. 1. A) A general map of the study area in the central Amazon Basin, B) Várzea do Lago Grande de Curuai with the TA14 sediment core site in the Santa Ninha Lake, and C) MAR2 and COM1 sediment core sites in Maracá and Comprido Lakes.

Fig. 2. Chemical structures of branched GDGTs and crenarchaeol considered in this study.

Fig. 3. Age–depth models for TA14, MAR2 and COM1 sediment cores, constructed based on the linear interpolation using the software Bacon (Blaauw and Christen, 2011).

Fig. 4. Lithological description of the TA14, MAR2 and COM1 sediment cores. Note that the TA14 and MAR2 cores were collected in the lakes directly connected to the Amazon River, while the COM1 core site was indirectly connection to the Amazon River. The grey bars indicate Unit II and the non-grey bare fields correspond to Unit I.

Fig. 5. TOC (wt. %), crenarchaeol (μg g_{TOC}^{-1}), summed branched GDGTs (i.e. the sum of the main branched GDGT Ia, IIa, andIIIa) (μg g_{TOC}^{-1}), the BIT index, and clay fraction (%) for A) TA14, B) MAR2, and C) COM1 sediment cores.

Fig. 6. Scatter plot of $\delta^{13}C_{TOC}$ (‰ VPDB) and C:N atomic ratio of the cores TA14, MAR2, and COM1. The boundaries of major OM sources are adapted from Kim et al. (2012).

Fig. 7. The methylation index of branched tetraethers (MBT), the degree of cyclization (DC), reconstructed pH, and MBT/CBT-derived MAAT for A) TA14, B) MAR2, and C) COM1 sediment cores.

Fig. 8. Scatter plot of A) the methylation index of branched tetraethers (MBT) versus the degree of cyclization (DC) and B) reconstructed pH vs reconstructed MAAT using the regional calibrations (Bendle et al., 2010) for comparison of branched GDGT distributions of TA14, MAR2, and COM1 cores with those of Amazon soils (Kim et al., 2012; Zell et al., 2013a) and Amazon River SPM (Zell et al., 2013b).

Table 1.

Sediment core	Depth (cm)	Lab internal number	^{14}C years BP ± analytical error	Calibrated ages (cal years BP, 2 sigma)	Mean calibrated age (cal years BP)
TA14	24	SacA3265	525 ± 69	344-663	530
	30	SacA5575	590 ± 30	514-629	545
	34	SacA3266	2313 ± 81	2049-2678	2300
	57	SacA5576	3335 ± 50	3395-3639	3560
	69	SacA5577	3000 ± 30	2994-3228	3100
	144	SacA8753	3920 ± 30	4159-4417	4350
	150	SacA8754	4525 ± 35	4975-5298	5200
	159	SacA3267	4354 ± 30	4832-4968	4850
	184	SacA3268	4430 ± 30	4856-5211	4950
	186	SacA3269	4455 ± 92	4842-5301	5000
	198	SacA3270	4510 ± 94	4853-5436	5200
	224	SacA3271	4588 ± 73	4964-5465	5300
	257	SacA3272	4549 ± 81	4872-5443	5260
	268	SacA5579	4900 ± 30	5482-5657	5600
MAR2	22	SacA 10680	260 ± 30	150-320	300
	37	SacA 10681	1980 ± 30	1823-1995	1880
	53	SacA 10682	1850 ± 30	1618-1827	1720
	62	SacA 21011	2080 ± 30	1924-2086	2000
	66	SacA 25868	1980 ± 35	1755-1997	1880
	75	SacA 21012	3065 ± 30	3078-3345	3300
	83	SacA 10683	3395 ± 30	3479-3690	3600
COM1	2	SacA25863	225 ± 30	0-300	150
	19	SacA10669	345 ± 30	305-455	325
	43	SacA10670	1005 ± 30	797-930	900
	69	SacA10671	1865 ± 30	1632-1833	1720
	92	SacA10672	2945 ± 30	2929-3163	3000
	94	SacA24996	7050 ± 45	7718-7943	7850
	120	SacA10673	9000 ± 30	9920-10224	10200

Fig. 1

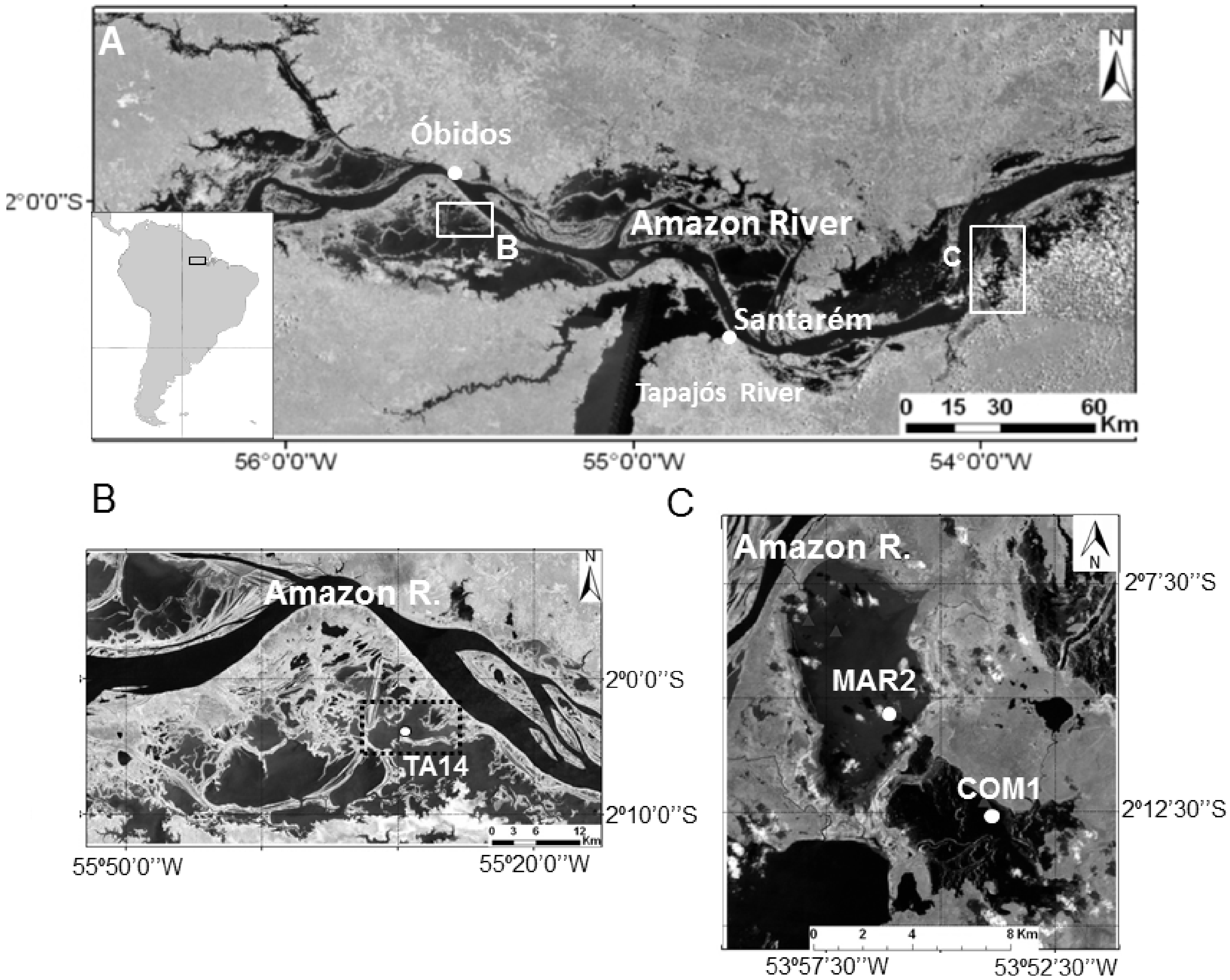
A
Óbidos
Amazon River
B
C
Santarém
Tapajós River
0 15 30 60
Km
N
2°0'0"S
56°0'0"W
55°0'0"W
54°0'0"W
B
Amazon R.
TA14
2º0'0''S
2º10'0''S
55º50'0''W
55º20'0''W
0 3 6 12 Km
N
C
Amazon R.
MAR2
COM1
2º7'30''S
2º12'30''S
53º57'30''W
53º52'30''W
0 2 4 8 Km
N

Fig. 2

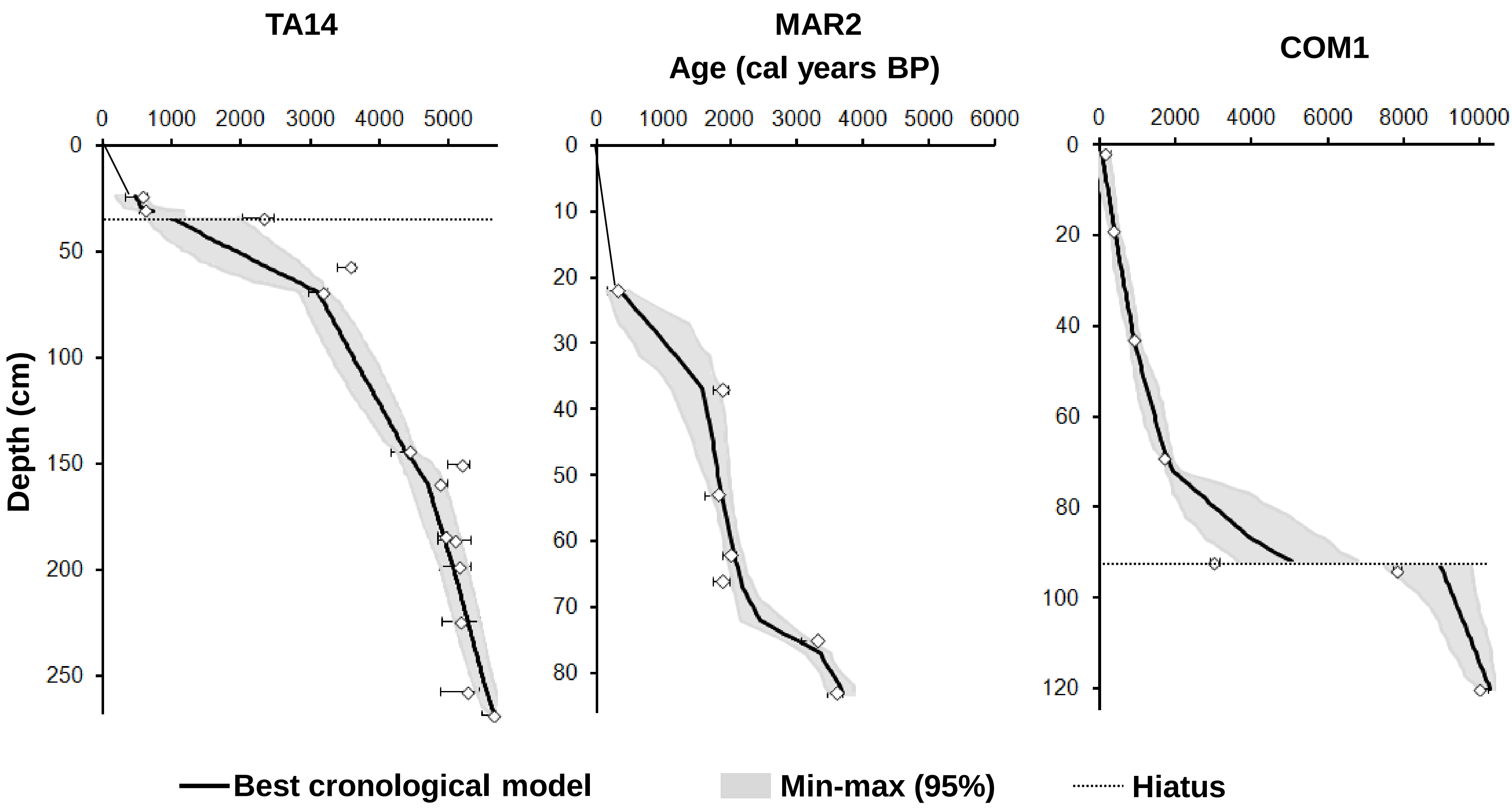

TA14
MAR2
Age (cal years BP)
COM1
0 1000 2000 3000 4000 5000
0 1000 2000 3000 4000 5000 6000
0 2000 4000 6000 8000 10000
Depth (cm)
0 50 100 150 200 250
0 10 20 30 40 50 60 70 80
0 20 40 60 80 100 120
Best cronological model
Min-max (95%)
Hiatus

Fig. 3

Ia

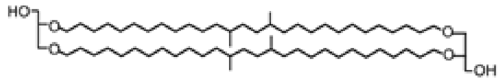

Ib

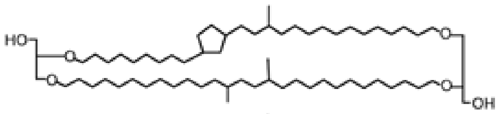

Ic

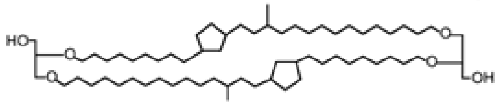

IIa

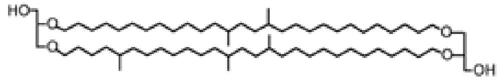

IIb

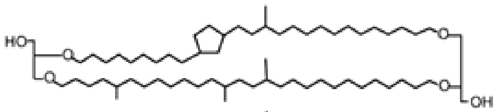

IIc

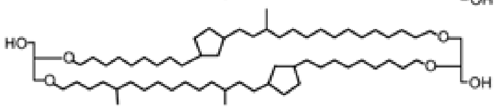

IIIa

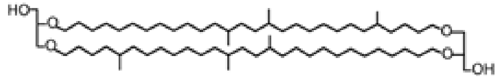

IIIb

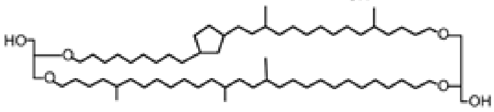

IIIc

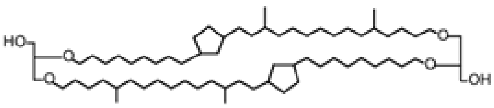

IV

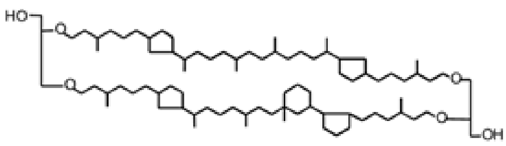

Fig. 4

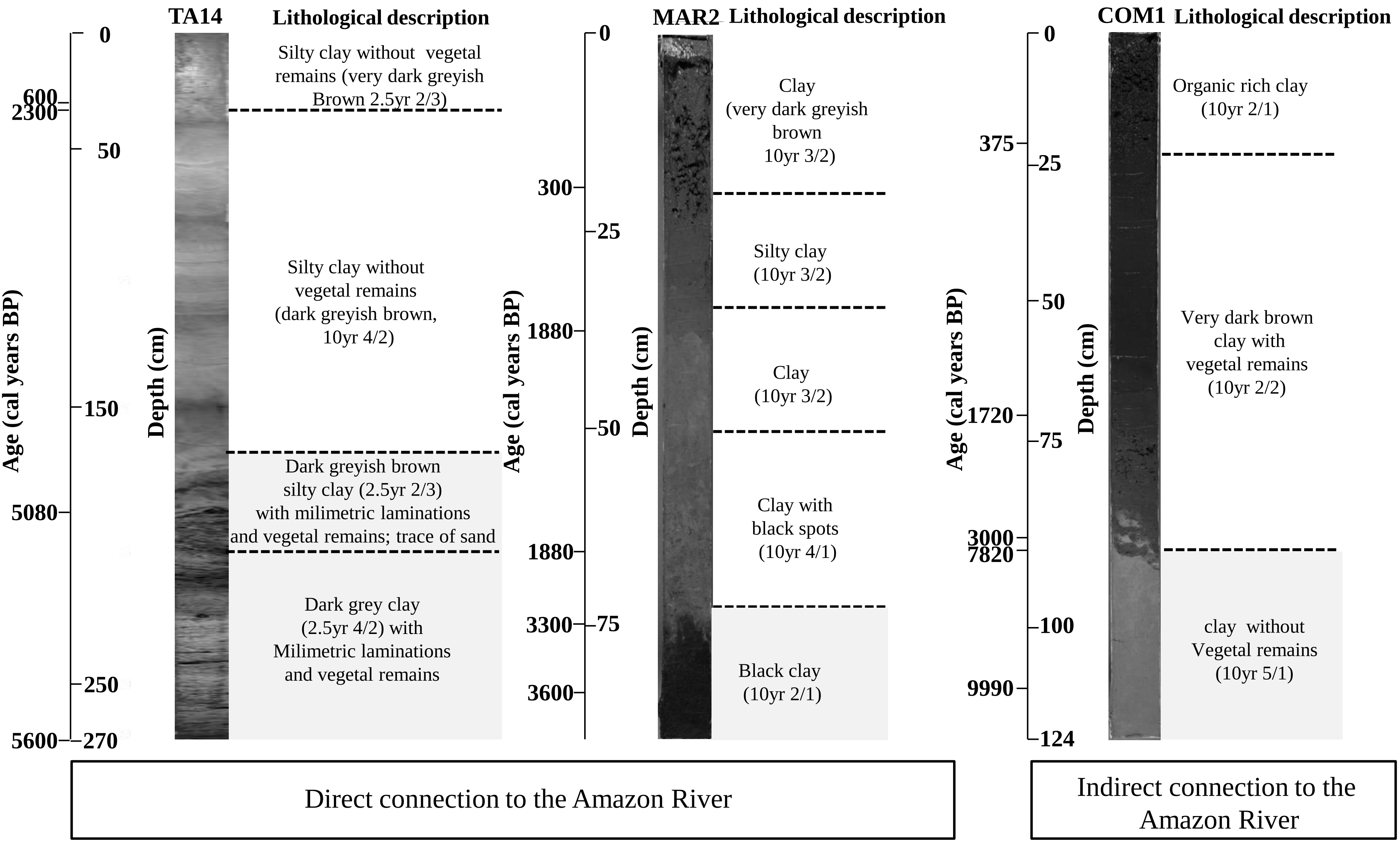

TA14
Lithological description
Silty clay without vegetal remains (very dark greyish Brown 2.5yr 2/3)
Silty clay without vegetal remains (dark greyish brown, 10yr 4/2)
Dark greyish brown silty clay (2.5yr 2/3) with milimetric laminations and vegetal remains; trace of sand
Dark grey clay (2.5yr 4/2) with Milimetric laminations and vegetal remains
Age (cal years BP)
Depth (cm)
0
600
2300
50
150
5080
250
5600
270
MAR2
Lithological description
Clay (very dark greyish brown 10yr 3/2)
Silty clay (10yr 3/2)
Clay (10yr 3/2)
Clay with black spots (10yr 4/1)
Black clay (10yr 2/1)
Age (cal years BP)
Depth (cm)
0
300
25
1880
50
1880
3300
75
3600
COM1
Lithological description
Organic rich clay (10yr 2/1)
Very dark brown clay with vegetal remains (10yr 2/2)
clay without Vegetal remains (10yr 5/1)
Age (cal years BP)
Depth (cm)
0
375
25
50
1720
75
3000
7820
100
9990
124
Direct connection to the Amazon River
Indirect connection to the Amazon River

Fig. 5

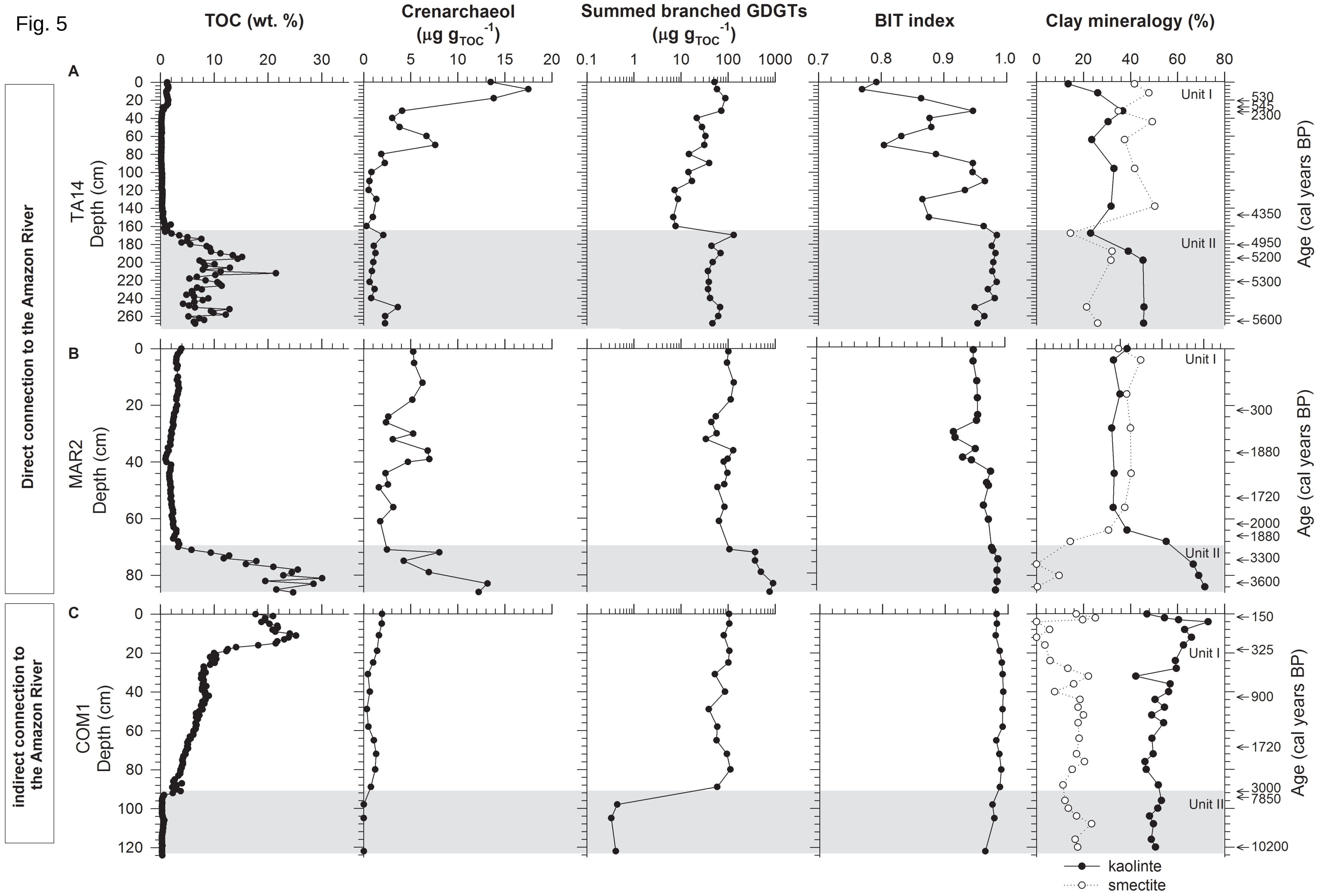
TOC (wt. %)
Crenarchaeol (µg g$_{TOC}^{-1}$)
Summed branched GDGTs (µg g$_{TOC}^{-1}$)
BIT index
Clay mineralogy (%)
A
B
C
Direct connection to the Amazon River
indirect connection to the Amazon River
TA14 Depth (cm)
MAR2 Depth (cm)
COM1 Depth (cm)
Age (cal years BP)
Unit I
Unit II
530
545
2300
4350
4950
5200
5300
5600
300
1880
1720
2000
1880
3300
3600
150
325
900
1720
3000
7850
10200
kaolinte
smectite

Fig. 6

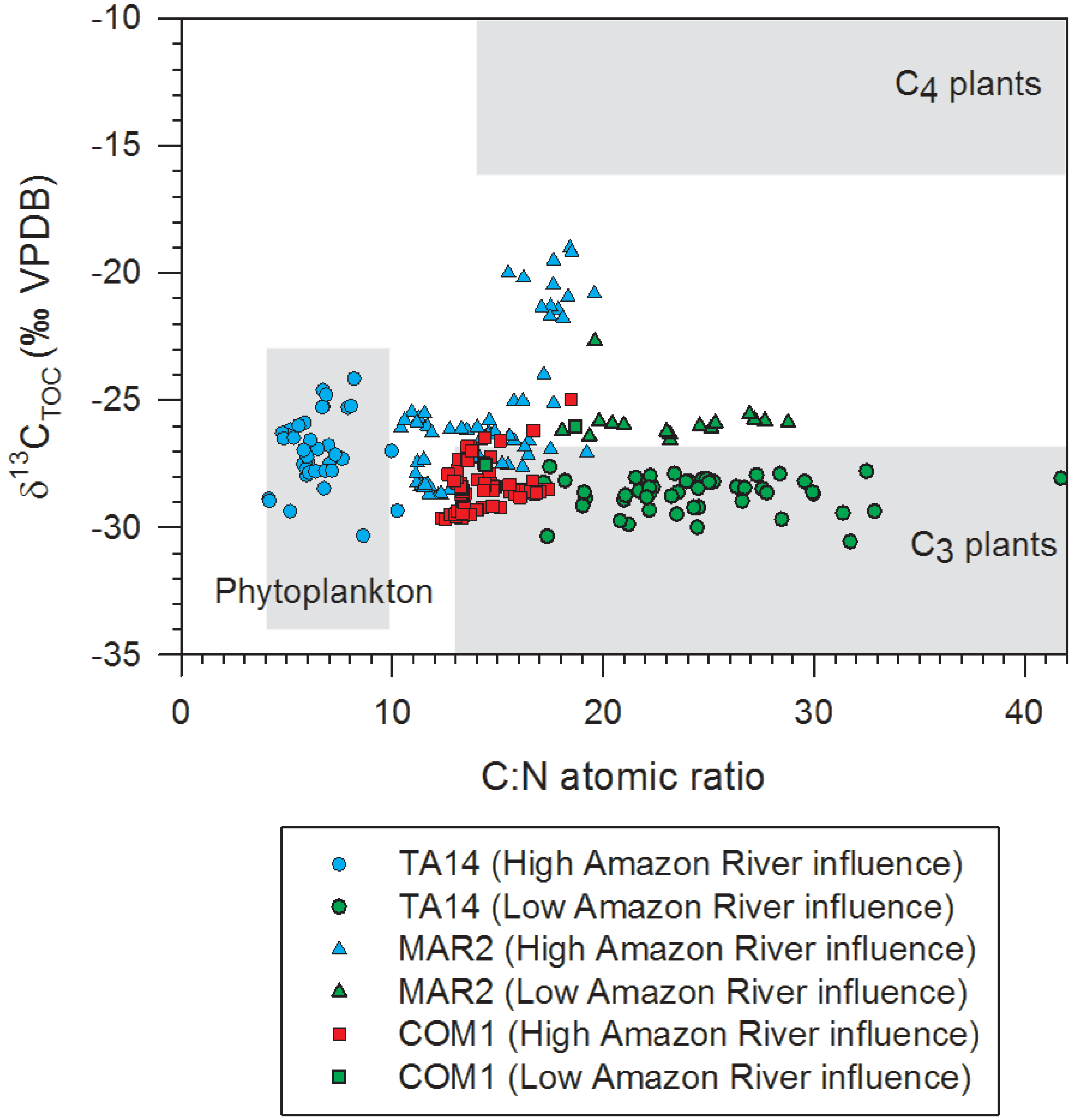

-10
-15
-20
-25
-30
-35
δ13CTOC (‰ VPDB)
0
10
20
30
40
C:N atomic ratio
C4 plants
C3 plants
Phytoplankton
TA14 (High Amazon River influence)
TA14 (Low Amazon River influence)
MAR2 (High Amazon River influence)
MAR2 (Low Amazon River influence)
COM1 (High Amazon River influence)
COM1 (Low Amazon River influence)

Fig. 7

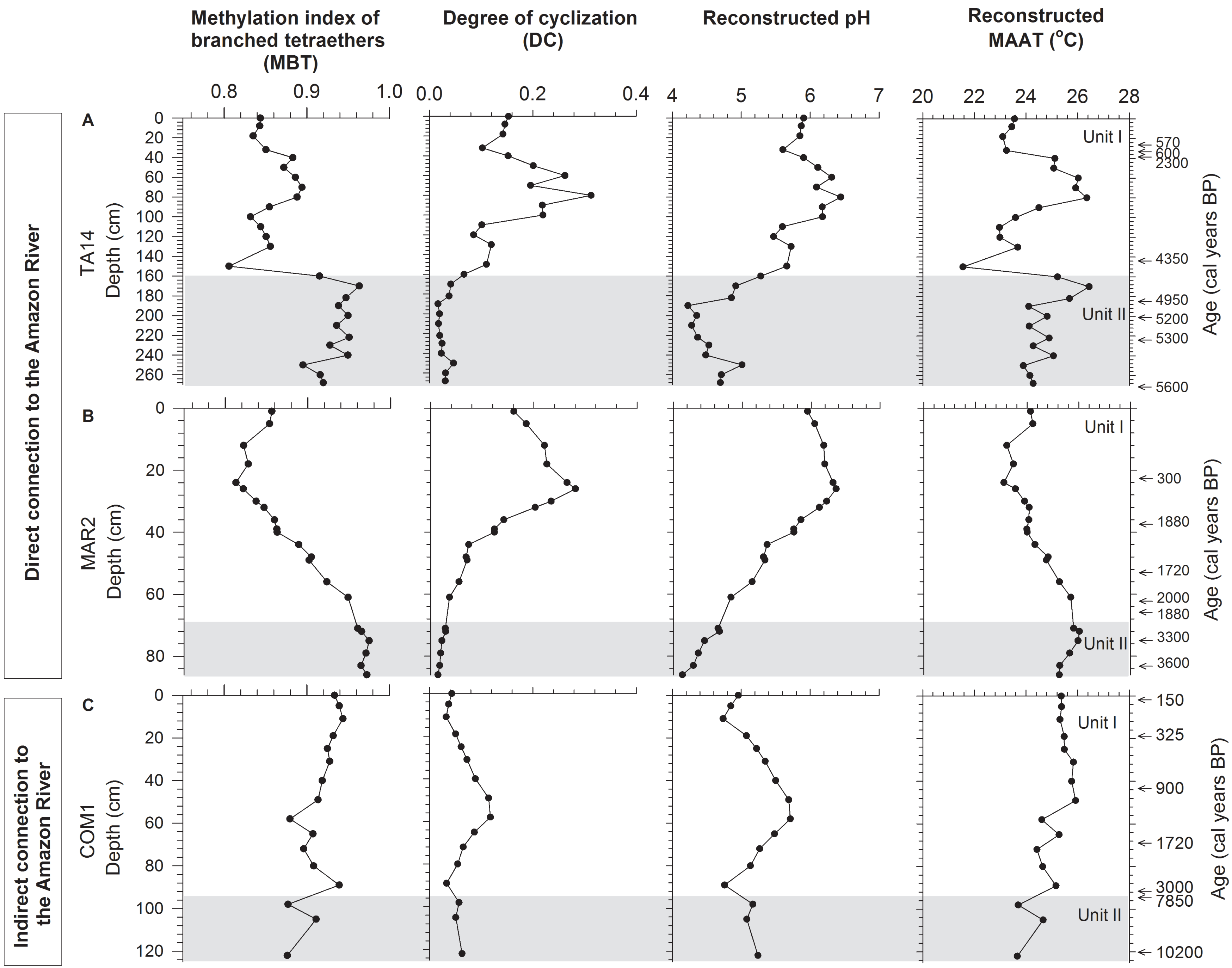

Methylation index of branched tetraethers (MBT)
Degree of cyclization (DC)
Reconstructed pH
Reconstructed MAAT (°C)
Direct connection to the Amazon River
Indirect connection to the Amazon River
A
B
C
TA14 Depth (cm)
MAR2 Depth (cm)
COM1 Depth (cm)
Unit I
Unit II
Age (cal years BP)
570
600
2300
4350
4950
5200
5300
5600
300
1880
1720
2000
1880
3300
3600
150
325
900
1720
3000
7850
10200

Fig. 8

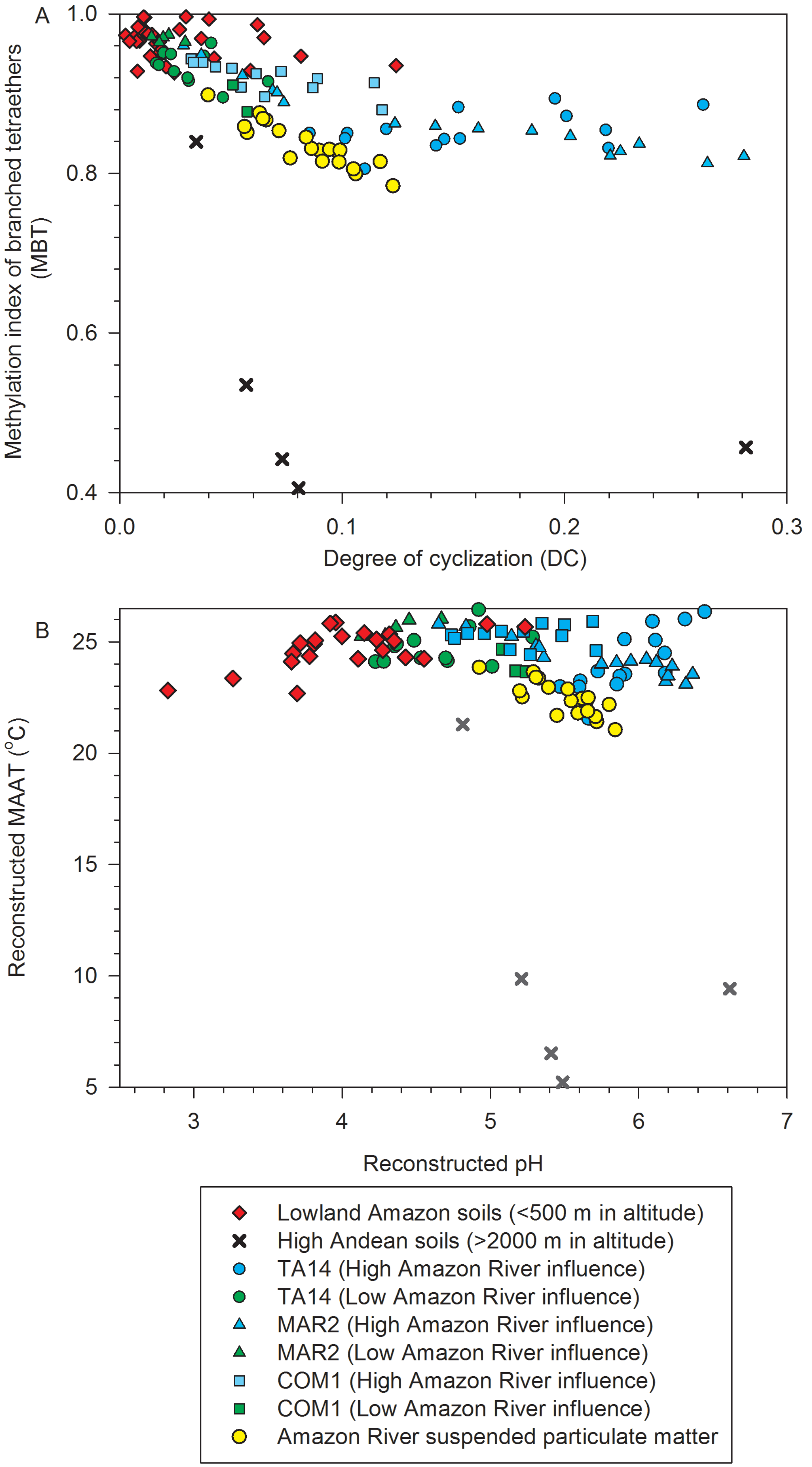
A
Methylation index of branched tetraethers (MBT)
1.0
0.8
0.6
0.4
0.0
0.1
0.2
0.3
Degree of cyclization (DC)
B
Reconstructed MAAT (°C)
25
20
15
10
5
3
4
5
6
7
Reconstructed pH
Lowland Amazon soils (<500 m in altitude)
High Andean soils (>2000 m in altitude)
TA14 (High Amazon River influence)
TA14 (Low Amazon River influence)
MAR2 (High Amazon River influence)
MAR2 (Low Amazon River influence)
COM1 (High Amazon River influence)
COM1 (Low Amazon River influence)
Amazon River suspended particulate matter